Atmospheric
Chemistry
and Physics

Variation in global chemical composition of PM$_{2.5}$: emerging results from SPARTAN

Graydon Snider[1], Crystal L. Weagle[2], Kalaivani K. Murdymootoo[1], Amanda Ring[1], Yvonne Ritchie[1], Emily Stone[1], Ainsley Walsh[1], Clement Akoshile[3], Nguyen Xuan Anh[4], Rajasekhar Balasubramanian[5], Jeff Brook[6], Fatimah D. Qonitan[7], Jinlu Dong[8], Derek Griffith[9], Kebin He[8], Brent N. Holben[10], Ralph Kahn[10], Nofel Lagrosas[11], Puji Lestari[7], Zongwei Ma[12], Amit Misra[13], Leslie K. Norford[14], Eduardo J. Quel[15], Abdus Salam[16], Bret Schichtel[17], Lior Segev[18], Sachchida Tripathi[13], Chien Wang[19], Chao Yu[20], Qiang Zhang[8], Yuxuan Zhang[8], Michael Brauer[21], Aaron Cohen[22], Mark D. Gibson[23], Yang Liu[20], J. Vanderlei Martins[24], Yinon Rudich[18], and Randall V. Martin[1,2,25]

[1]Department of Physics and Atmospheric Science, Dalhousie University, Halifax, Nova Scotia, Canada
[2]Department of Chemistry, Dalhousie University, Halifax, Nova Scotia, Canada
[3]Department of Physics, University of Ilorin, Ilorin, Nigeria
[4]Institute of Geophysics, Vietnam Academy of Science and Technology, Hanoi, Vietnam
[5]Department of Civil and Environmental Engineering, National University of Singapore, Singapore
[6]Department of Public Health Sciences, University of Toronto, Toronto, Ontario, Canada
[7]Faculty of Civil and Environmental Engineering, ITB, JL. Ganesha No.10, Bandung, Indonesia
[8]Center for Earth System Science, Tsinghua University, Beijing, China
[9]Council for Scientific and Industrial Research (CSIR), Pretoria, South Africa
[10]Earth Science Division, NASA Goddard Space Flight Center, Greenbelt, MD, USA
[11]Manila Observatory, Ateneo de Manila University, Quezon City, Philippines
[12]School of Environment, Nanjing University, Nanjing, China
[13]Center for Environmental Science and Engineering, Indian Institute of Technology Kanpur, Kanpur, India
[14]Department of Architecture, Massachusetts Institute of Technology, Cambridge, MA, USA
[15]UNIDEF (CITEDEF-CONICET) Juan B. de la Salle 4397 – B1603ALO Villa Martelli, Buenos Aires, Argentina
[16]Department of Chemistry, University of Dhaka, Dhaka, Bangladesh
[17]Cooperative Institute for Research in the Atmosphere, Colorado State University, Fort Collins, CO, USA
[18]Department of Earth and Planetary Sciences, Weizmann Institute of Science, Rehovot, Israel
[19]Center for Global Change Science, Massachusetts Institute of Technology, Cambridge, MA, USA
[20]Rollins School of Public Health, Emory University, 1518 Clifton Road NE, Atlanta, GA, USA
[21]School of Population and Public Health, University of British Columbia, Vancouver, British Columbia, Canada
[22]Health Effects Institute, 101 Federal Street Suite 500, Boston, MA, USA
[23]Department of Process Engineering and Applied Science, Dalhousie University, Halifax, Nova Scotia, Canada
[24]Department of Physics and Joint Center for Earth Systems Technology, University of Maryland, Baltimore County, Baltimore, MA, USA
[25]Harvard-Smithsonian Center for Astrophysics, Cambridge, MA, USA

Correspondence to: Graydon Snider (graydon.snider@dal.ca) and Randall V. Martin (randall.martin@dal.ca)

Abstract. The Surface PARTiculate mAtter Network (SPAR-TAN) is a long-term project that includes characterization of chemical and physical attributes of aerosols from filter samples collected worldwide. This paper discusses the ongoing efforts of SPARTAN to define and quantify major ions and trace metals found in fine particulate matter (PM$_{2.5}$). Our methods infer the spatial and temporal variability of PM$_{2.5}$ in a cost-effective manner. Gravimetrically weighed filters represent multi-day averages of PM$_{2.5}$, with a collocated nephelometer sampling air continuously. SPARTAN instruments are paired with AErosol RObotic NETwork (AERONET) sun photometers to better understand the relationship between ground-level PM$_{2.5}$ and columnar aerosol optical depth (AOD).

We have examined the chemical composition of PM$_{2.5}$ at 12 globally dispersed, densely populated urban locations and a site at Mammoth Cave (US) National Park used as a background comparison. So far, each SPARTAN location has been active between the years 2013 and 2016 over periods of 2–26 months, with an average period of 12 months per site. These sites have collectively gathered over 10 years of quality aerosol data. The major PM$_{2.5}$ constituents across all sites (relative contribution $\pm$ SD) are ammoniated sulfate (20 % $\pm$ 11 %), crustal material (13.4 % $\pm$ 9.9 %), equivalent black carbon (11.9 % $\pm$ 8.4 %), ammonium nitrate (4.7 % $\pm$ 3.0 %), sea salt (2.3 % $\pm$ 1.6 %), trace element oxides (1.0 % $\pm$ 1.1 %), water (7.2 % $\pm$ 3.3 %) at 35 % RH, and residual matter (40 % $\pm$ 24 %).

Analysis of filter samples reveals that several PM$_{2.5}$ chemical components varied by more than an order of magnitude between sites. Ammoniated sulfate ranges from 1.1 µg m^{-3} (Buenos Aires, Argentina) to 17 µg m^{-3} (Kanpur, India in the dry season). Ammonium nitrate ranged from 0.2 µg m^{-3} (Mammoth Cave, in summer) to 6.8 µg m^{-3} (Kanpur, dry season). Equivalent black carbon ranged from 0.7 µg m^{-3} (Mammoth Cave) to over 8 µg m^{-3} (Dhaka, Bangladesh and Kanpur, India). Comparison of SPARTAN vs. coincident measurements from the Interagency Monitoring of Protected Visual Environments (IMPROVE) network at Mammoth Cave yielded a high degree of consistency for daily PM$_{2.5}$ ($r^2 = 0.76$, slope $= 1.12$), daily sulfate ($r^2 = 0.86$, slope $= 1.03$), and mean fractions of all major PM$_{2.5}$ components (within 6 %). Major ions generally agree well with previous studies at the same urban locations (e.g. sulfate fractions agree within 4 % for 8 out of 11 collocation comparisons). Enhanced anthropogenic dust fractions in large urban areas (e.g. Singapore, Kanpur, Hanoi, and Dhaka) are apparent from high Zn : Al ratios.

The expected water contribution to aerosols is calculated via the hygroscopicity parameter κ_{v} for each filter. Mean aggregate values ranged from 0.15 (Ilorin) to 0.28 (Rehovot). The all-site parameter mean is 0.20 ± 0.04. Chemical composition and water retention in each filter measurement allows inference of hourly PM$_{2.5}$ at 35 % relative humidity by merging with nephelometer measurements. These hourly PM$_{2.5}$ estimates compare favourably with a beta attenuation monitor (MetOne) at the nearby US embassy in Beijing, with a coefficient of variation $r^2 = 0.67$ ($n = 3167$), compared to $r^2 = 0.62$ when κ_{v} was not considered. SPARTAN continues to provide an open-access database of PM$_{2.5}$ compositional filter information and hourly mass collected from a global federation of instruments.

1   Introduction

Fine particulate matter with a median aerodynamic diameter less than or equal to 2.5 µm (PM$_{2.5}$) is a robust indicator of premature mortality (Chen et al., 2008; Laden et al., 2006). Research on long-term exposure to ambient PM$_{2.5}$ has documented serious adverse health effects, including increased mortality from chronic cardiovascular disease, respiratory disease, and lung cancer (WHO, 2005). Outdoor fine particulate matter (PM$_{2.5}$) is recognized as a significant air pollutant, with an air quality guideline set by the WHO at 10 µg m^{-3} annual average (WHO, 2006). Many regions of the world far exceed these long-term recommendations (Brauer et al., 2015; van Donkelaar et al., 2015), and the impact on health is substantial. The 2013 Global Burden of Disease estimated that outdoor PM$_{2.5}$ caused 2.9 million deaths (3 % of all deaths) and 70 million years of lost healthy life on a global scale (Forouzanfar et al., 2015). Atmospheric aerosol is also the most uncertain agent contributing to radiative forcing of climate change (IPCC, 2013). Aerosol mass and composition also play a critical role in atmospheric visibility (Malm et al., 1994). Additional observations are needed to improve the concentration estimates for PM$_{2.5}$ as a global risk factor, and to better understand the chemical components and sources contributing to its formation.

The chemical composition of PM$_{2.5}$ offers valuable information to identify the contributions of specific sources, and to understand aerosol properties and processes that could affect health, climate, and atmospheric conditions. Spatial mapping of aerosol type and composition using satellite observations and chemical transport modelling can help elucidate the global exposure burden of fine particulate matter composition (Kahn and Gaitley, 2015; Lelieveld et al., 2015; Patadia et al., 2013; Philip et al., 2014a); however, ground-level sampling remains necessary to evaluate these estimates and provide quantitative details. Furthermore, the long-term health impacts of specific chemical components are not well understood (e.g. Lepeule et al., 2012). The health-related impacts of specific PM composition have been reviewed previously (Lippmann, 2014). Although PM$_{2.5}$ composition can be implicated in the variance observed in cardiovascular health effects, there is insufficient long-term PM$_{2.5}$ characterization for adequate health impact assessments of specific aerosol mixtures (e.g. Bell et al., 2007). More generally, ur-

ban PM$_{2.5}$ speciation is not yet consistently characterized on a global scale. Continental sampling has been conducted in North America (Hand et al., 2012) and Europe (Putaud et al., 2004, 2010), however, there remains a need for a global network that consistently measures PM$_{2.5}$ chemical composition in densely populated regions.

No global PM$_{2.5}$ protocol exists for relative humidity (RH) filter equilibration. The U.S. EPA measurements are between 30 and 40 % RH, European measurements are below 50 % RH, and different protocols exist elsewhere. Ambient humidity affects the relationship of dry PM$_{2.5}$ with satellite observations of aerosol optical depth. Aerosol water also influences the relationship between dry PM$_{2.5}$ and aerosol scatter. A large body of literature has examined the relationship of aerosol composition with hygroscopicity (e.g. IMPROVE (Hand et al., 2012; IMPROVE, 2015), Chemical Species Network (CSN) (Chu, 2004; USEPA, 2015), ISORROPIA (Fountoukis and Nenes, 2007), and Aerosol Inorganic Model (AIM) (Wexler and Clegg, 2002)). More recently, Petters and Kreidenweis (2007, 2008, 2013) have developed κ-Kohler theory, which assigns individual hygroscopicity parameters κ to all major components, from insoluble crustal materials to sea salt. Mixed values can then be weighted by local aerosol composition.

Ground-based observations of PM$_{2.5}$ have insufficient coverage at the global scale to provide assessment of long-term human exposure. Satellite remote sensing offers a promising means of providing an extended temporal record to estimate population exposure to PM$_{2.5}$ on a global scale, and especially for areas with limited ground-level PM$_{2.5}$ measurements (Brauer et al., 2015; van Donkelaar et al., 2015). Even in areas where monitor density is high, satellite-based estimates provide additional useful information on spatial and temporal patterns in air pollution (Kloog et al., 2011, 2013; Lee et al., 2012). However, there are outstanding questions about the accuracy and precision with which ground-level aerosol mass concentrations can be inferred from satellite remote sensing. Standardized PM$_{2.5}$ measurements, collocated with ground-based measurements of aerosol optical depth, are needed to evaluate and improve PM$_{2.5}$ estimates from satellite remote sensing. To meet these sampling needs, the ground-based network SPARTAN (Surface PARTiculate mAtter Network) is designed to evaluate and enhance satellite-based estimates of PM$_{2.5}$ by measuring fine-particle aerosol concentrations and composition continuously over multi-year periods at sites where aerosol optical depth is also measured (Holben et al., 1998; Snider et al., 2015). The network includes air filter sampling and nephelometers that together provide long-term and hourly PM$_{2.5}$ estimates at low RH (35 %).

We discuss the ongoing efforts of the SPARTAN project to quantify major ions and trace metals found in aerosols worldwide. Section 2 describes the methodology used to infer PM$_{2.5}$ composition. Section 3 defines categories of aerosol types (crustal and residual material, equivalent black carbon, ammonium nitrate, ammoniated sulfate, sea salt, and trace metal oxides) as a function of specific chemical species. Section 4 describes the implementation of sub-saturated κ-Kohler theory to estimate aerosol water content based on aerosol compositional information. Section 5 compares relative aerosol composition with that reported in available literature, and assesses the general consistency of our findings across all sites. Section 6 evaluates hourly PM$_{2.5}$ estimates (35 % RH) at Beijing with a beta attenuation monitor at the US embassy.

2 Overview of methodology

SPARTAN has been collecting PM$_{2.5}$ on PTFE filters for at least 2 months, across 13 SPARTAN sites, between 2013 and 2016, with an average period of 12 months per site. Snider et al. (2015) provide an overview of the SPARTAN PM observation network, the cost-effective sampling methods employed and post-sampling instrumental methods of analysis. Each site utilizes a combination of continuous monitoring by nephelometry and mass concentration via filter-based sampling. Nephelometer scatter is averaged to hourly intervals at three wavelengths (457, 520, 634 nm), and converted to 550 nm via a fitted Angstrom exponent. Total scatter is proportional to PM$_{2.5}$ mass and volume (Chow et al., 2006). Hence, we provide dry (35 % RH) hourly PM$_{2.5}$ estimates by combining scatter at 550 nm at ambient RH with filter mass and chemical composition information used to determine water content as described below.

Briefly, filter-based measurements are collected with an AirPhoton SS4i automated air sampler. Each sampler houses a removable filter cartridge that protects seven sequentially active 25 mm diameter filters, plus a field blank. Air samples first pass through a bug screen and then a greased impactor plate to remove particles larger than 10 µm in diameter. Aerosols are collected in sequence on a preweighed Nuclepore filter membrane (8 µm, SPI) that removes coarse-mode aerosols with diameters from 2.5 to 10 µm in diameter (PM$_c$), while fine aerosols (PM$_{2.5}$) are then collected on pre-weighed PTFE filters (2 µm, SKC). For each filter, sampling is timed at regular, staggered 24 h intervals throughout a 9-day period. Sampling ends for each filter at 09:00 LT when temperatures are low, to reduce loss of semi-volatile components. As described by Snider et al. (2015), loss rates of ammonium nitrate during passive air flow were an order of magnitude less than during active air flow. Thus, the sampling protocol is designed to actively sample for one diurnal cycle and to avoid daytime sampling after collecting nighttime PM. Following the IMPROVE protocol (Hand and Malm, 2006), filters are transported at room temperature in sealed containers between measurement sites and the central SPARTAN laboratory at Dalhousie University, where analysis is conducted.

Site locations are designed to sample under a variety of conditions, including biomass burning (e.g. west Africa and South America), biofuel emissions (e.g. south Asia), monsoonal conditions (e.g. west Africa and southeast Asia), suspended mineral dust (e.g. west Africa and the Middle East) and urban crustal material. Each SPARTAN site provides a representative example of local and regional conditions in highly populated areas. Site selection prioritizes underrepresented, globally dispersed, population-dense regions; no SPARTAN sites exist yet in Europe. The sites of Atlanta and Mammoth Cave are included for instrument intercomparison purposes with other networks.

2.1 Filter weighing

Filters (PTFE, capillary) are both pre and post-weighed in triplicate using a Sartorius Ultramicro balance with 0.1 μg precision. Gravimetric weighing is performed in a cleanroom facility at 35 ± 5 % RH and 20–23 °C. A total of 497 quality-controlled filters have been weighed across all SPARTAN sites. The median collected material on sampled filters, as well as the lower and upper quintiles (in parentheses), are 72 (42, 131) μg for Teflon and 90 (44, 154) μg for Nuclepore. The combined uncertainty ($\pm 2\sigma$) of quality-assured single-filter PM mass measurements is ±4.0 μg. Time-integrated flow rates at ambient air pressure and temperature are used to define the sampled volume for aerosol concentrations reported in μg m^{-3}. These filters are subsequently analysed for water-soluble ions, trace metals, and surface reflectance to obtain equivalent black carbon.

2.2 Equivalent black carbon (EBC)

We define the equivalent black carbon (EBC) as the black carbon content of PTFE filters derived via surface reflectance R using the Diffusion Systems EEL 43M smoke stain reflectometer (Quincey et al., 2009) as further discussed in Sect. 4.6. We use the term "equivalent black carbon" following the recommendation of Petzold et al. (2013) for data derived from optical absorption methods.

2.3 Trace metals

To maximize the information extracted from the filters, each one is cut in half with a ceramic blade following approaches similar to Zhang et al. (2013) and Gibson et al. (2009). One filter half is analysed for crustal components Mg, Fe, and Al as well as trace elements Zn, V, Ni, Cu, As, Se, Ag, Cd, Sb, Ba, Ce, and Pb. We first digest this filter half by adding it to 3.0 mL of 7 % trace-metal-grade nitric acid, similar to Fang et al. (2015). The acid–filter combination is boiled at 97 °C for 2 h, and the liquid extract is submitted for quantitative analysis via inductively coupled plasma mass spectrometry (ICP-MS, Thermo Scientific X-Series 2), and follows standardized methodology as in Rice et al. (2012). The ICP-MS analysis is quantified via five concentrations (25, 50, 100,

250, and 500 μg L^{-1}) of a 25-element acidified stock solution. Three reference metal ions (^{45}Sc, ^{115}In, and ^{159}Tb) are also used for atomic mass calibration. All ion mass signals are measured in triplicate, and the mean signal value is used for elemental quantification.

2.4 Water-soluble ions

Water-soluble ions NO_3^-, SO_4^{2-}, NH_4^+, K^+Na^+ are detected using the second filter half. The filter is spiked with 120 μL of isopropyl alcohol and immersed in 2.9 mL of 18 MΩ Milli-Q water. Filters and liquid extracts are sonicated together for 25 min before being passed through a 0.45 μm membrane filter to remove larger matrix components. Extractions are analysed by ion chromatography (IC) via a Thermo Dionex ICS-1100 instrument (anions) and a Thermo Dionex ICS-1000 (cations) instrument (Gibson et al., 2013a, b).

3 PM$_{2.5}$ aerosol composition

Section 2 defined the methodology of basic physical and chemical properties obtained in SPARTAN filters. Section 3 describes the chemical definitions used to infer each chemical component as discussed in turn below. Table 1 contains a summary of equations and accompanying references used to quantify SPARTAN PM$_{2.5}$ chemical composition.

3.1 Sea salt (SS)

We take 10 % of [Al] to be associated with Na and remove this crustal sodium component (Remoundaki et al., 2013). Sea salt is then represented as 2.54[Na$^+$]$_{ss}$ to account for the associated [Cl$^-$] (Malm et al., 1994).

3.2 Ammonium nitrate (ANO$_3$)

We treat all nitrate as neutralized by ammonium as NH$_4$NO$_3$. The corresponding mass of ANO$_3$ is a 1 : 1 molar ratio of NH$_4$: NO$_3$, or 1.29[NO$_3^-$] based on molecular weight.

3.3 Sodium sulfate (Na$_2$SO$_4$)

Sodium sulfate is treated as a fraction of measured sodium, 0.18[Na$^+$]$_{SS}$ (Henning et al., 2003); however, it contributes negligibly to total aerosol mass (< 0.1 %) at all sites.

3.4 Ammoniated sulfate (ASO$_4$)

Ammonium not associated with nitrate and sulfate not associated with sodium are assumed to be associated as a mixture of NH$_4$HSO$_4$ and (NH$_4$)$_2$SO$_4$.

3.5 Crustal material (CM)

Crustal material consists of resuspended road dust, desert dust, soil, and sand. Following the elemental composition of

Table 1. Summary of speciation definitions.

Species (at 0 % RH)	Measurement method	Species mass (µg) (for concentrations, divide masses by sampling volume v)	Reference
SS	IC (anion and cation)	$2.54[\text{Na}^+]_{\text{SS}}$, where $[\text{Na}^+]_{\text{SS}} = [\text{Na}^+]_{\text{tot}} - 0.1[\text{Al}]$	Remoundaki et al. (2013), Malm et al. (1994)
ANO$_3$		$1.29[\text{NO}_3^-]$	Malm et al. (1994)
ASO$_4$		$[\text{SO}_4^{2-}]_{\text{non-ss}} + [\text{NH}_4^+] - 0.29[\text{NO}_3^-]$, where $[\text{SO}_4^{2-}]_{\text{non-ss}} = [\text{SO}_4^{2-}]_{\text{tot}} - 0.12[\text{Na}^+]$	Dabek-Zlotorzynska et al. (2011), Henning et al. (2003)
Na$_2$SO$_4$		$0.18[\text{Na}^+]_{\text{SS}}$	
CM	ICP-MS	$10 \times ([\text{Al}] + [\text{Mg}] + [\text{Fe}])$	Wang (2015)
EBC	SSR	$20.7 \times \ln (R_0/R)$	Taha et al. (2007)
TEO	ICP-MS	$1.47[\text{V}] + 1.27[\text{Ni}] + 1.25[\text{Cu}] + 1.24[\text{Zn}] + 1.32[\text{As}] + 1.2[\text{Se}] + 1.07[\text{Ag}] + 1.14[\text{Cd}] + 1.2[\text{Sb}] + 1.12[\text{Ba}] + 1.23[\text{Ce}] + 1.08[\text{Pb}]$	Malm et al. (1994)
PBW$_{\text{inorg}}$	$\kappa_{\text{m},X}$	$\sum_X [1/f_{\text{m},X}(\text{RH}) - 1][X]$	Kreidenweis et al. (2008)
PBW$_{\text{RM}}$		$\text{RM}(1 - 1/f_{\text{m,RM}})$	Table 2
RM(35 %)	Mass balance	$[\text{PM}_{2.5}] - \{ [\text{EBC}] + [\text{CM}] + [\text{TEO}] + [\text{ANO}_3] + [\text{SS}] + [\text{ASO}_4] + [\text{Na}_2\text{SO}_4] + [\text{PBW}]_{\text{inorg}} \}$	This study
RM(0 %)	Mass balance $\kappa_{\text{m,OM}} = 0.07$	$\text{RM}(35 \%) - \text{PBW}_{\text{RM}}$	Organic growth factors: Jimenez et al. (2009), Sun et al. (2011)

Species: EBC indicates equivalent black carbon, TEO indicates trace metal oxides, CM indicates crustal material, ANO$_3$ indicates ammonium nitrate, ASO$_4$ indicates ammoniated sulfate, PBW indicates particle-bound water, RM indicates residual matter (assumed representative of organic matter), [X] indicates concentration of any hygroscopic species. Measurement instruments: IC indicates ion chromatography, ICP-MS indicates inductively coupled plasma mass spectrometry, SSR indicates smoke stain reflectometer, $\kappa_{\text{m},X}$ indicates single-parameter hygroscopicity by mass (Kreidenweis et al., 2008). RH indicates relative humidity.

natural desert dusts by Wang (2015), we generalize that natural CM is approximately $10 \times [\text{Al} + \text{Fe} + \text{Mg}]$. Aluminum, iron, and magnesium are chosen due to their collectively consistent composition in natural mineral dust and frequency above detection limit ($> 95\,\%$). Silicon is not available. Titanium was found not to contribute significantly ($< 1\,\%$) to CM mass.

3.6 Equivalent black carbon (EBC)

The amount of EBC carbon (µg) is logarithmically related to concentration, as determined by relative surface reflectance R/R_0. For a given exposed filter area, absorption cross section and light path, reflectance is related to concentration via

$$[\text{EBC}] = \frac{-A}{qv}\ln\left(\frac{R}{R_0}\right), \tag{1}$$

where v is volume of air (0.9–$5.8\,\text{m}^3$), A is the filter surface area ($3.1\,\text{cm}^2$), and q is the product of the effective reflectivity path p and mass-specific absorption cross section σ_{SSR} ($\text{cm}^2\,\text{µg}^{-1}$). The absorption coefficient σ_{SSR} used here is $0.06\,\text{cm}^2\,\text{µg}^{-1}$ based on prior literature (Barnard et al., 2008; Bond and Bergstrom, 2006), adjusted to the 620 nm detection peak of the SSR. The effective light path p here is taken to be 1.5 for our thick PTFE filters (e.g. Taha et al., 2007). We treat water uptake by EBC as negligible.

3.7 Trace elemental oxides (TEO)

Trace elemental oxides are the summation of estimated oxide mass for trace elements as measured by ICP-MS, and make up a negligible portion of total mass ($< 1\,\%$). We include these concentrations for completeness. Water uptake by TEO is treated as negligible.

3.8 Particle-bound water (PBW) associated with inorganics

We estimate the water-mass uptake for the inorganic chemical components of sea salt (SS), ammonium nitrate (ANO$_3$), and ammoniated sulfate (ASO$_4$). The mass of particle-bound water (PBW) associated with chemical component X is

$$\text{PBW}_X = [X]\kappa_{\text{m},X}\frac{\text{RH}}{100 - \text{RH}}. \tag{2}$$

The total mass of inorganic (IN) PBW is then $\text{PBW}_{\text{IN}} = \sum_X \text{PBW}_X$.

3.9 Residual matter (RM)

Residual matter, which is treated as mainly organics, is estimated by subtracting dry inorganic mass (IN) and its associated water (referenced to our weighing conditions of $35 \pm 5\,\%$ RH) from total PM$_{2.5}$ mass:

$$RM_{35\%} = PM_{2.5,35\%} - [IN] - [PBW_{IN}]. \tag{3}$$

Negative $RM_{35\%}$ values are retained if reconstructed inorganic mass at 35 % RH exceeds total PM$_{2.5}$ by less than 10 %, otherwise values are flagged and excluded from the mass average. Negative values occur, on average, 2 % of the time. Water-free RM (0 % RH) is estimated by subtracting organic-associated PBW using an estimated hygroscopic parameter $\kappa_{m,RM} = 0.1$ as discussed in Sect. 4.

4 Aerosol hygroscopicity

We apply the single-parameter measure of aerosol hygroscopicity (κ) developed by Petters and Kreidenweis (2007, 2008, 2013) to represent the contribution of water uptake by individual components. The κ parameter is defined from 0 (insoluble materials) to greater than 1 for sea salt. Although initially developed for supersaturated CCN conditions, hygroscopic parameters κ have been more recently used in sub-saturated conditions (Chang et al., 2010; Dusek et al., 2011; Giordano et al., 2013; Hersey et al., 2013). For particle diameters that dominate the mass fraction of PM$_{2.5}$ (larger than 50 nm), the difference in κ between CCN and sub-saturated aerosols is small (Dusek et al., 2011). The water retention of internal mixtures of aerosol components is often predicted within experimental error (Kreidenweis et al., 2008). Aged, polarized organic material, which is a major component of PM$_{2.5}$, shows comparable growth factors both in super- and sub-saturated regions (Rickards et al., 2013).

The volume hygroscopicity parameter κ_v is defined as a function of particle volume V and water activity a_w:

$$\frac{1}{a_w} = 1 + \kappa_v \frac{V_d}{V_w}, \tag{4}$$

where V_d and V_w are the dry particulate matter and water volumes, respectively. To a first-order approximation $a_w = RH/100$. Aerosol volume growth is related via κ and RH by defining $f_v(RH)$ as the humidity-dependent ratio of wet and dry aerosol volume:

$$f_v(RH) \equiv \frac{V_{tot}}{V_d} = \frac{V_d + V_w}{V_d} = a + \kappa_v \frac{RH}{100 - RH}. \tag{5}$$

Combining the previous equations and relating to a diameter D growth factor (GF $\equiv D/D_d$) yields

$$GF = \left(a + \kappa_v \frac{RH}{100 - RH}\right)^{1/3}, \tag{6}$$

where $a = 1$, except for sea salt, as discussed in Sect. 3.1. Reliable estimates of κ_v are available for individual components (cf. Table 2).

The next sections outline how we apply κ to represent mass and volume hygroscopic growth in major hygroscopic aerosol components. Four components directly contribute to water uptake: ammonium nitrate (ANO$_3$), ammoniated sulfate (ASO$_4$), sea salt (SS), and organics. We treat black carbon (EBC), crustal material (CM), and trace oxides (TEO) as non-hygroscopic. We evaluated inorganic component growth curves using the AIM model (Wexler and Clegg, 2002) for RH = 10–90 % except for sea salt, which included RH = 0 %. Hygroscopic parameters were matched to modelled fits. Aerosols are treated as internally mixed, without deliquescence or efflorescence points, as discussed further below.

4.1 Inorganic behaviour

Figure 1 shows the hygroscopic growth for inorganics. The κ_v value of 0.51 for ammonium sulfate best matches the AIM model over RH = 10–90 % and is similar to the GF-derived $\kappa_v = 0.53$ estimated by Petters and Kreidenweis (2007). The κ_v value for ammonium bisulfate is similar to the κ_v value of ammonium sulfate, which is adopted here for ASO$_4$. Our AIM-derived ammonium nitrate growth curve is smaller than ammonium sulfate, at $\kappa_v = 0.41$. Empirically, both ammonium compounds share the same GF = 1.6 at RH = 85 % (Sorooshian et al., 2008), however, ANO$_3$ is less hygroscopic at lower RH.

Sea salt accounts for a small fraction of aerosol mass over land, however, its hydrophilic nature makes it significant for water retention. A 1 : 1 volume ratio with water as RH approaches 0 % (Kreidenweis et al., 2008) yields $a = 2$ (Eqs. 2 and 3). A hygroscopic constant $\kappa_v = 1.5$ then best fits AIM from the deliquescence point up to 90 % RH.

We follow the widely used convention (e.g. Pitchford et al., 2007) that PM$_{2.5}$ under variable sub-saturated RH does not exhibit deliquescent phase transitions. There is compelling evidence to adopt smooth hygroscopic growth curves. Various experiments show sub-micrometer, internally mixed aerosols will not deliquesce as readily as pure compounds. For example, Badger et al. (2006) observed ASO$_4$ aerosol deliquescence is clearly inhibited by the presence of humic acids. A smooth growth curve has been observed over the range RH = 10–85 % for ambient aerosols at Jungfraujoch (Swietlicki et al., 2008). Analysis of sub-micron aerosol mixtures consisting of SS, ASO$_4$, ANO$_3$, and levoglucosan also showed no apparent phase transition (Svenningsson et al., 2006).

4.2 Organic matter behaviour

Identifying a representative organic hygroscopic parameter is challenging, as many volume growth curves are available based on a variety of laboratory experiments and field campaigns. Organic composition varies by site, and by season. The Appendix Table Al contains a collection of hygroscopic parameters from the literature. Values for $\kappa_{v,OM}$ range from 0 to 0.2. We choose a single $\kappa_{v,OM}$ value based on the oxygen/carbon ratio (O : C), which is a function of oxidation,

Table 2. The κ-Kohler constants for volume (κ_{v}), mass (κ_{m}), and related quantities.

Compound [X]	$\kappa_{\mathrm{v},X}$	Approximate density ($\rho_X / \rho_{\mathrm{water}}$)	$\kappa_{\mathrm{m},X}$	PBW(% mass) at RH = 35 %	RH = 80 %
Crustal	0	2.5[a]	0	0	0
EBC	0	1.8[b]	0	0	0
TEO	0	2.5	0	0	0
RM	0.1[c]	1.4	0.07	2	12
ANO$_3$	0.41	1.72	0.24	17	61
ASO$_4$	0.51	1.76	0.29	15	56
Na$_2$SO$_4$	0.68[d]	2.68[d]	0.25	12	50
SS	1.5[e]	2.16	0.69	22	68

PBW indicates particle-bound water. EBC indicates equivalent black carbon, TEO indicates trace element oxides, RM indicates residual matter (associated with organics), ANO$_3$ indicates ammonium nitrate, ASO$_4$ indicates ammoniated sulfate. [a] Wagner et al. (2009). [b] Bond and Bergstrom (2006). [c] Assuming an urban O : C ratio of 0.5, then $\kappa_{\mathrm{v,OM}} = 0.1$, Jimenez et al. (2009). [d] Petters and Kreidenweis (2007). [e] Fitted using non-deliquesced, sub-saturated AIM Model III values, plus 0 % RH endpoint by Kreidenweis et al. (2008).

hence age of the organics. Generally O : C ratios are between 0.2 and 0.8 in urban environments (Rickards et al., 2013). We select an O : C ratio of 0.5 to represent the populated nature of SPARTAN sites (e.g. Robinson et al., 2013). This corresponds to an organic parameter of $\kappa_{\mathrm{v,OM}} = 0.1$ for a variety of organic mixtures (Jimenez et al., 2009).

4.3 Aerosol water in multi-component systems

Mass-based hygroscopic water uptake κ_{m} is more convenient than κ_{v} to estimate water retention in gravimetric analysis. The parameters κ_{v} and κ_{m} are related by water-normalized density, $\kappa_{\mathrm{m},X} = \kappa_{\mathrm{v},X}/\rho_X$. Table 2 contains κ_{v} values identified for major aerosol chemical components and densities. For a multi-component system we estimate aerosol water mass using a mass-weighted combination of κ_{m} values:

$$\kappa_{\mathrm{m,tot}} = \frac{1}{M}\sum_X m_X \kappa_{\mathrm{m},X}. \tag{7}$$

Mass calculations are used to determine residual aerosol mass as described in Sect. 3.9. Estimates of total water uptake by volume are applied to aerosol light scatter in Sect. 5. The volume parameter $\kappa_{\mathrm{v,tot}}$ is similarly determined by a linear combination of volume-weighted components X (e.g. Bezantakos et al., 2013):

$$\kappa_{\mathrm{v,tot}} = \frac{1}{V}\sum_X v_X \kappa_{\mathrm{v},X}. \tag{8}$$

The hygroscopic growth of ASO$_4$ and organic mixtures are treated as linear combinations of pure compounds (Robinson et al., 2013). Errors in aerosol water uptake are less significant in mixtures than for individual species due to dilution effects (Kreidenweis et al., 2008). For ambient aerosols, empirically measured $\kappa_{\mathrm{v,tot}}$ usually lies between 0.14 and 0.39 (Carrico et al., 2010).

4.4 Sources of uncertainty

Uncertainty in atmospheric PM$_{2.5}$ concentrations can be separated into air volume and PM$_{2.5}$ mass. We estimated total flow volume variance to be ± 10 %, while 2σ pre- and post-gravimetric mass measurement varied by a combined $\pm 4\,\mu\mathrm{g}$. Characterization of hourly PM$_{2.5}$ uncertainties can be found in Appendix A2.

Of concern is the loss of semi-volatiles after sampling. In the laboratory semi-volatile loss is inhibited by storing filters in closed containers. As discussed in Sect. 2, the sampling protocol is designed to minimize semi-volatile loss. We tested the retention of semi-volatile material in the field by examining the trend in PM$_{2.5}$ and ANO$_3$ mass from the first filter sampled (54-day residence time in instrument) through the last filter sampled (negligible residence time in instrument). Statistically insignificant trends were found for both PM$_{2.5}$ ($-0.09 \pm 0.46\,\mu\mathrm{g\,m}^{-3}$ position^{-1}) and ANO$_3$ ($0.06 \pm 0.15\,\mu\mathrm{g\,m}^{-3}$ position^{-1}), providing confidence in retention of semi-volatiles on filters in the cartridge.

Other uncertainties include absolute equivalent black carbon mass due to the reflectivity path p (± 30 %) and absorption cross section σ (± 30 %), which combine to (in quadrature) ± 42 %. Trace metal recovery yields were tested using a sequential second digestion with 20 % nitric acid. Each acid-digested element was quantified by five dilutions of a 25-element standard (25–500 ppb), plus three internal calibration metals (Sc, In, Tb). The elemental comparison of crustal materials varies regionally (Wang, 2015), which contributes to CM uncertainty of ± 30 % based on Al, Fe, and Mg composition. Recovery of individual water-soluble elements was determined through five-point anion and cation standards curves each with $r^2 > 98$ % and < 10 % mass uncertainty for most elements at environmentally relevant concentrations, including sulfate, nitrate, and ammonium. Based on lab filter spike tests, water-soluble ion extractions show > 95 % extraction efficiency. Uncertainties of water-soluble
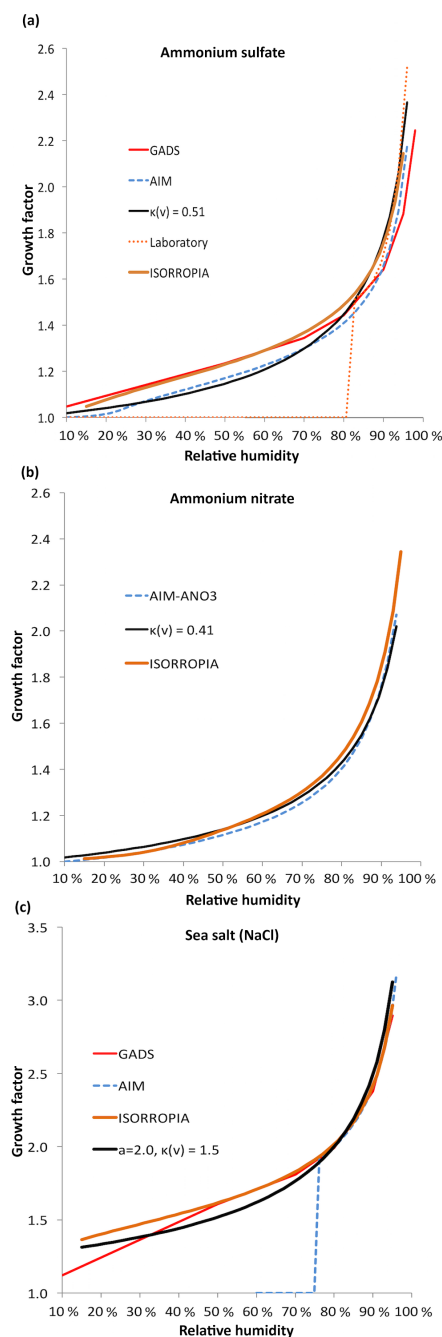
Figure 1. Hygroscopic growth factors for ammonium sulfate (top), ammonium nitrate (centre), and sea salt (bottom). GADS = Global Aerosol Data Set estimated from empirical data (Koepke et al., 1997). ISORROPIA indicates aerosol thermodynamic model at $T = 298$ K (reverse mode) and assuming linear water/solvent volume additivity (Fountoukis and Nenes, 2007). AIM = Aerosol Inorganic Model calculated metastable growth for ammonium sulfate and ammonium nitrate at $T = 298$ K (Wexler and Clegg, 2002). Laboratory ammonium sulfate fit is GF $= 149 + 281 \cdot$ RH$^{24.6}$ (with deliquescence at 80 %) for bulk pure ammonium sulfate (Wise et al., 2003). All components are fit using Eq. (6).

ion yields are generally ±5 %, except when close to the limit of detection (approximately 0.1 µg m^{-3}, depending on filter sampling duration). Errors in the component values affect our estimate of κ_v, which will affect the inferred aerosol water. Network evaluation is an ongoing task that will continue over time.

5 Mass speciation results

5.1 Overview of PM$_{2.5}$ mass speciation

Gravimetrically weighed PM$_{2.5}$ concentrations within the period June 2013–February 2016 span an order of magnitude, from under 10 µg m^{-3} (e.g. Atlanta) to almost 100 µg m^{-3} (Kanpur). Sites include a variety of geographic regions including partial desert (Ilorin, Rehovot, Kanpur), coastline (Buenos Aires, Singapore), and developing megacities (Dhaka). Table 3 and Fig. 2 contain the resulting PM$_{2.5}$ mass, composition, and location of each SPARTAN site. The mean SPARTAN composition over all sampling sites in descending concentration is 40 % RM (primarily organic), 20 % ASO$_4$, 13 % CM, 12 % EBC, 4.7 % ANO$_3$, 2.3 % SS, and 1.0 % TEO.

There is significant variation of relative and absolute speciation from these long-term averages. ASO$_4$ concentrations range from 1 µg m^{-3} (Buenos Aires, summer) to 17 µg m^{-3} (Kanpur, dry season). The fraction of sulfate in PM$_{2.5}$ exhibits much weaker spatial variation (10–30 %) as increases in ASO$_4$ coincide with increases in total PM$_{2.5}$. Hence, locations with enhanced sulfate tend to have enhancements in other aerosol components.

ANO$_3$ concentrations exhibit a larger spatial heterogeneity than sulfate. Absolute values range over 30-fold, from 0.2 µg m^{-3} (Mammoth Cave, summer) to 6.8 µg m^{-3} (Kanpur, dry season). Corresponding mass fractions are 7–8 % in Kanpur, Beijing, and Buenos Aires, and below 2 % in Bandung. This heterogeneity reflects large spatial and temporal variation in NH$_3$ and NO$_x$ (NO + NO$_2$) sources. There were noticeable seasonal increases in ANO$_3$ during wintertime periods in Beijing, Kanpur, and Dhaka, coinciding with lower temperatures.

CM concentrations span an order of magnitude from 1.0 µg m^{-3} (Atlanta) to 16 µg m^{-3} (Beijing). The fraction of CM in PM$_{2.5}$ exhibits pronounced variation (5–25 %). Except during dust storms, CM does not show clear patterns of temporal or regional variation. This could be explained by non-seasonal road dust, which may account for over 80 % of CM in regions with heavy urban traffic (Huang et al., 2015).

We used Zn : Al ratios to assess the relative importance of local road dust (cf. Table 3). Aluminum is mostly natural in origin (Zhang et al., 2006), whereas Zn is primarily from tire wear (Begum et al., 2010; Councell et al., 2004). For example, ratios are above 3 for Dhaka and Hanoi, but less than 0.3 for Mammoth Cave and the South Dekalb site (Atlanta).

Table 3. PM$_{2.5}$ composition and water content (μg m^{-3}) at each SPARTAN location.

City	Host institute	Lat/long (°)	Elev./Inst. Elev. (m)	Filters (n)	ASO$_4$	ANO$_3$	CM	SS	EBC	TEO	RM	PBW 35%RH	ρ 0%RH (g cm^{-3})	NO$_3$ vs. NH$_4^+$ (r^2)	PM$_{2.5}$	$\frac{PM_{2.5}}{PM_{10}}$	$\kappa_{V,tot}$	PM$_{2.5}$ $\frac{K}{Al}$	$\frac{Zn}{Al}$	Filter sampling period
Beijing	Tsinghua University	40.010, 116.333	60// 7.5	114	12.0ᵃ (7.9)	5.5 (6.4)	15.9 (8.8)	1.5 (2.1)	5.7 (3.4)	0.62 (0.51)	23.8 (18)	4.7 (2.8)	1.69	0.32	69.5 (2.5)	0.49	0.19	2.9	0.51	2013/06–2016/02
Bandung	ITB Bandung	−6.888, 107.610	826// 20	77	6.0 (2.3)	0.7 (1.3)	2.5 (1.5)	0.3 (0.2)	3.7 (2.0)	0.14 (0.11)	16.0 (5.9)	1.9 (0.6)	1.55	0.06	31.4 (1.0)	0.58	0.17	6.8	0.52	2014/01–2015/11
Manila	Manila Observatory	14.635, 121.080	60// 10	63	2.7 (1.5)	0.3 (0.2)	1.9 (1.0)	0.5 (0.4)	4.3 (3.3)	0.13 (0.13)	7.3 (3.5)	1.1 (0.5)	1.61	0.03	18.2 (0.8)	0.39	0.16	6.3	1.03	2014/02–2016/01
Dhaka	Dhaka University	23.728, 90.398	20// 20	41	7.5 (4.3)	2.1 (1.8)	5.9 (4.0)	1.4 (1.7)	8.4 (5.1)	1.50 (1.46)	21.4 (16)	3.5 (2.2)	1.63	0.43	51.9 (3.7)	0.40	0.17	5.3	3.39	2014/05–2015/11
Ilorin	Ilorin University	8.484, 4.675	330// 10	40	1.9 (0.8)	0.3 (0.1)	3.0 (2.2)	0.3 (0.4)	1.6 (0.8)	0.09 (0.07)	7.6 (3.8)	0.9 (0.4)	1.62	0.05	15.7 (0.8)	0.44	0.15	2.9	0.49	2014/03–2015/10
Kanpur	IIT Kanpur	26.519, 80.233	130// 10	33	17.6 (12)	6.8 (5.3)	4.4 (2.3)	0.6 (0.3)	8.3 (4.7)	0.47 (0.36)	54.6 (33)	6.3 (3.6)	1.52	0.58	99.3 (9.1)	0.56	0.18	16.2	1.01	2013/12–2014/11
Buenos Aires	CITEDEF	−34.560, −58.506	25// 7	31	1.1 (0.5)	0.8 (0.4)	2.2 (1.6)	0.6 (0.3)	1.7 (1.2)	0.12 (0.12)	3.1 (1.8)	0.9 (0.3)	1.70	0.28	10.1 (0.6)	0.39	0.19	2.7	0.44	2014/10–2016/02
Rehovot	Weizmann Institute	31.907, 34.810	20// 10	30	4.7 (1.9)	0.9 (0.5)	3.3 (1.6)	0.7 (0.6)	2.2 (2.0)	0.12 (0.13)	2.6 (2.8)	1.6 (0.6)	1.79	0.01	16.1 (1.0)	0.40	0.28	2.7	0.40	2015/02–2016/02
Mammoth Cave NP	Mammoth Cave	37.132, −86.148	235// 7	19	4.1 (2.4)	0.2 (0.1)	1.4 (1.4)	0.1 (0.1)	0.7 (0.4)	0.02 (0.03)	6.1 (4.3)	1.0 (0.5)	1.59	0.00	13.6 (1.8)	0.56	0.22	1.1	0.13	2014/04–2014/08
Atlanta	Emory University	33.688, −84.290	250// 2	13	2.0 (0.9)	0.3 (0.1)	1.0 (0.4)	0.1 (0.1)	1.1 (1.0)	0.04 (0.02)	4.1 (1.8)	0.6 (0.2)	1.61	0.00	9.1 (0.7)	0.69	0.17	1.9	0.26	2014/01–2014/05
Singapore	NUS	1.298, 103.780	10// 20	12	16.1 (6.5)	1.2 (0.9)	0.8 (0.3)	0.9 (0.4)	3.1 (2.7)	0.20 (0.16)	39.8 (29)	5.0 (2.4)	1.48	0.66	66.8 (11)	NA	0.21	13.2	1.53	2015/08–2015/12
Hanoi	Vietnam Acad. Sci.	21.048, 105.800	10// 20	10	6.0 (2.1)	1.6 (0.4)	5.6 (5.4)	0.9 (0.2)	3.7 (2.1)	0.69 (0.43)	18.2 (7.8)	2.6 (0.7)	1.59	0.22	39.4 (3.9)	0.38	0.18	8.9	3.74	2015/05–2015/08
Pretoria	CSIR	−25.756, 28.280	1310// 10	5	1.2 (1.6)	0.7 (0.3)	1.3 (1.8)	0.2 (0.1)	1.4 (0.9)	0.04 (0.04)	1.0 (0.7)	0.5 (0.4)	2.09	0.48	6.4 (2.3)	0.32	0.24	6.0	0.86	2015/09–2015/11
SPARTAN mean (% mass)	All sites			497	20 (11)%	4.7 (3.0)%	13.4 (9.9)%	2.3 (1.6)%	11.9 (8.4)%	1.0 (1.1)%	40 (24)%	7.2 (3.3)%	1.65	0.24	32.4 (2.9)	0.50	0.20	4.6ᵇ	0.73ᵇ	2013–2016

ᵃ Values in parentheses are 1σ standard deviations. RH indicates relative humidity. ANO$_3$ indicates ammonium nitrate. ASO$_4$ indicates ammoniated sulfate. CM indicates crustal material. EBC indicates equivalent black carbon. TEO indicates trace element oxides. RM indicates residual matter. PBW indicates particle-bound water. Mean Na$_2$SO$_4$ was not significant (<0.1 μg m^{-3}) at any SPARTAN site. ᵇ Geometric mean.

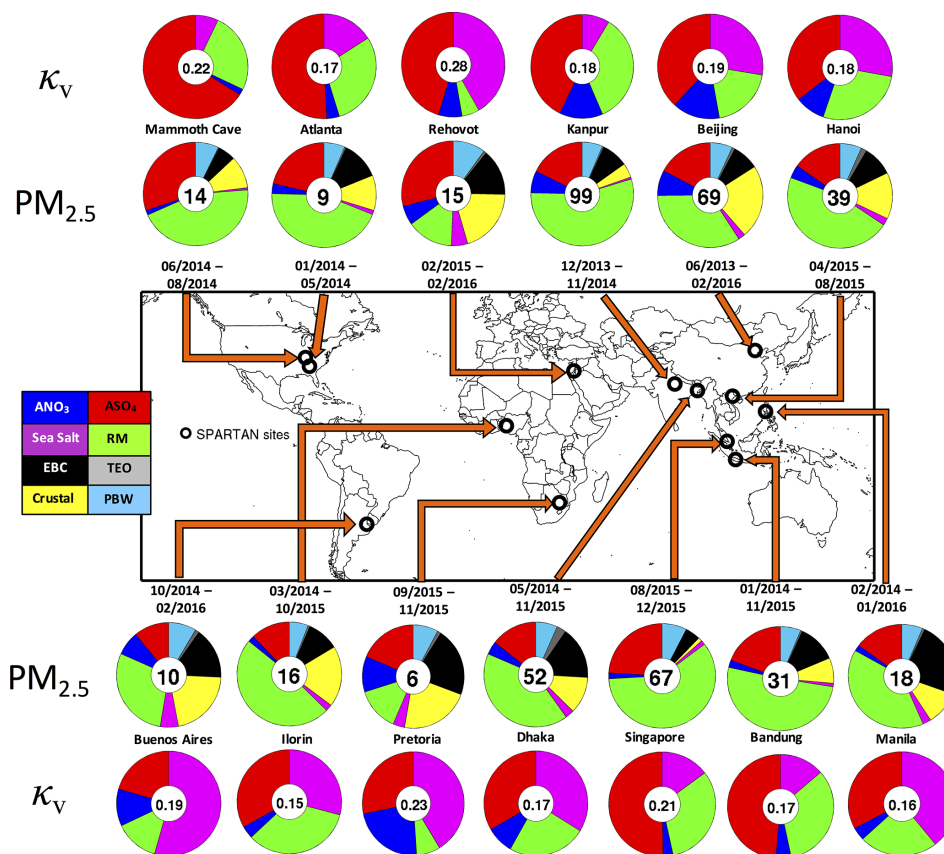**Figure 2.** PM$_{2.5}$ mass (inner circle, µg m^{-3}) and composition mass fraction (filled colours) is shown in interior pie charts. Exterior pie charts contain site-mean κ_v surrounded by the relative contribution of PBW water at 35 % RH.

In fine-mode aerosols, the ratio tends to be highest in large cities distant from natural CM. In coarse-mode aerosols, a low Zn : Al ratio (< 0.1) indicates the aerosol CM component is dominated by regional dust.

Absolute EBC spans an 8-fold concentration range from 1.1 µg m^{-3} (Atlanta) to above 8 µg m^{-3} (Dhaka and Kanpur). Mass fractions of EBC ranged from 4 % (Singapore) to 25 % (Manila). Trace element oxide (TEO) material is mainly composed of Zn, Pb, Ni, Cu, and Ba, hence also derived mainly from anthropogenic sources. TEO contributes negligibly to total mass (1 %), as expected. Sea salt remains a consistently small contributor (2 %) to total mass, except for Buenos Aires and Rehovot (5–6 %) due to coastal winds. Particle-bound water (PBW) mass at 35 % humidity is determined from the growth parameter κ_m. PBW mass contribution is similar to EBC (7 %). At low humidity, the combined mass of ANO$_3$, EBC, TEO, sea salt, and PBW accounts for 15–35 % of aerosol mass.

RM as inferred from mass reconstruction of inorganic compounds, PBW, and total filter-weighed mass is implicitly treated as the organic aerosol mass fraction. In terms of relative composition, RM spans a factor of 2, from 30 % mass in Buenos Aires to almost 60 % in Kanpur. Temporal changes

in RM tend to coincide with increases in ASO$_4$, with an all-site $r^2 = 0.92$. Although RM, as defined here, is not fully independent from measured ASO$_4$, correlations between these two mass fractions imply related sources.

We interpret the abundance of water-soluble K relative to Al as an indicator of wood smoke (e.g. Munchak et al., 2011). K : Al ratios averaged over each site range from < 2 (Mammoth Cave, Atlanta) to 16 (Kanpur), where combustion activity is apparent. Singapore was downwind of significant Indonesian forest fire smoke during its sampling period of August–November 2015, averaging to K : Al $= 13$. The correlation between K : Al and RM across all SPARTAN sites is $r^2 = 0.73$, supporting the attribution of RM as mostly organic.

Across all sites, coarse- and fine-mode mass fractions are approximately equal (0.50), with fractions ranging from below 0.40 (Hanoi, Buenos Aires, Manila) to above 0.55 (e.g. Bandung, Kanpur, Atlanta, Mammoth Cave). The two size modes can be temporally correlated per site, though sometimes weakly, from $r^2 = 0.15$ (Hanoi) to $r^2 = 0.76$ (Rehovot). We observe strong temporal correlations between sulfate and ammonium in PM$_{2.5}$ ($r^2 = 0.72$–0.99). Nitrate and ammonium are less consistently related (Table 3), rang-

ing from higher values in Singapore ($r^2 = 0.66$), Kanpur ($r^2 = 0.58$), Beijing ($r^2 = 0.28$), to weaker values in Ilorin and Manila ($r^2 < 0.1$). The strength of correlations with ammonium could be influenced by excess ammonium relative to sulfate. The $\left[NH_4^+ \right] / [SO_4^{2-}]$ ratio in PM$_{2.5}$ is 2.6 in Kanpur and 1.3 in Ilorin.

5.2 Collocation overview

We compare SPARTAN PM$_{2.5}$ speciation with previous studies available from the literature and focus on collocated relative PM$_{2.5}$ composition of major components within the last 10 years. TEO is omitted due to lack of significant mass contribution. Aerosol water content is also omitted as it was not directly measured in any of the collocation studies. If not provided, CM is treated as defined in Sect. 4.5 where possible. Organic mass (OM) to organic carbon (OC) ratios are from Philip et al. (2014b) with updates from Canagaratna et al. (2015).

Figure 3 provides an overview of the comparison studies organized by SPARTAN data availability. Only sampling at Mammoth Cave was temporally coincident with the comparison data. SPARTAN compositional information is generally consistent with previous studies, considering inter-annual chemical variation and measurement uncertainty. For example, both SPARTAN and comparative studies find that PM$_{2.5}$ is composed of between 10 and 30 % ASO$_4$ and 5–20 % CM for sampled sites. SPARTAN EBC mass fraction generally matches within 5 percentage points of collocated studies, except for Bandung and Kanpur. SPARTAN and prior studies find that ANO$_3$ is usually a small fraction of total mass, except at Beijing and Kanpur (7–8 %) due to their high agricultural and industrial activity. All studies find that sea salt is below 3 % of total mass. SPARTAN-derived RM has potentially the largest potential error, yet typically is consistent with the combined organic and unknown masses of other studies. This offers further evidence that SPARTAN measurements of RM are predominantly organic in nature.

5.3 Individual site characteristics

Below, we discuss each site in more detail. We also examine how our chemical composition from a global array of sites relates to local anthropogenic activities and surrounding area. References to land type at specific sites are derived from Latham et al. (2014), unless otherwise indicated. The number of filters is given in parentheses.

5.3.1 Beijing, China ($n = 114$)

Beijing has attracted considerable attention for its air pollution (Chen et al., 2013). Agricultural areas to the west and the Gobi Desert to the north surround the city's 19 million dwellers. The SPARTAN air sampler is located on the Tsinghua University campus, 15 km northwest of the downtown centre. This is our longest-running site, with 2.5 years of

near-continuous sampling. It reports the third-highest PM$_{2.5}$, at 69 µg m^{-3}, the third-highest ASO$_4$ (12 µg m^{-3}), and the highest CM (16 µg m^{-3}) of all sites. The significant ANO$_3$ (5.5 µg m^{-3}) reflects significant urban NO$_x$ near agricultural NH$_3$ sources. ANO$_3$ values were highest during winter, as expected from ammonium-nitrate thermodynamics. A high CM component in the springtime reflects regional, natural CM sources. The mean PM$_{2.5}$ Zn : Al ratio is lower than in other large cities (0.51) likely due to a larger fraction of natural dust sources and the sampling location in the northwest quadrant of the city, upwind of many traffic sources. The lowest coarse-mode Zn : Al mass ratios are observed in April 2014 (0.07) and April 2015 (0.06) during the annual yellow dust storm season. This is balanced by urban dust sources throughout the year, in agreement with Lin et al. (2015) who found evidence of high CM in industrial areas of Beijing.

The Beijing comparison showed that relative masses in Beijing compare well with previous studies. SPARTAN ASO$_4$ (19 %) is close to Yang et al. (2011) (17 %) and Oanh et al. (2006) (20 %), and the RM of 37 % is similar to combined OM (33 and 29 %) and unknown fractions (10 and 24 %) of comparison studies. SPARTAN ANO$_3$ concentrations (8.5 %) are relatively higher than for most other locations, though lower than in either previous study (11–12 %), possibly due to different sampling periods. CM is greater than in Yang et al. (2011) (25 % vs. 19 %), and significantly higher than in Oanh et al. (2006) (5 %), potentially due to a difference in definitions.

5.3.2 Bandung, Indonesia ($n = 77$)

Bandung is located inland on western Java surrounded by a volcanic mountain range and agriculture (e.g. tea plantations). The sampler is located on the Institute of Technology Bandung campus, 5 km north of the city centre. Almost 2 years of sampling have resulted in a mean PM$_{2.5}$ concentration of 31 µg m^{-3}. Sea salt is low at this elevated (826 m) inland site. ANO$_3$ and CM levels are also low, but RM is moderately high compared with other sites, at 55 %. This could be explained by large amounts of vegetative burning; organic PM$_{2.5}$ mass fractions can rise above 70 % during combustion episodes (Fujii et al., 2014). Volcanic sources of sulfur, in addition to industrial sources, may explain the relatively higher ASO$_4$ compared with Manila or Dhaka (Lestari and Mauliadi, 2009). Influxes of volcanic dust from the Sinabang volcano from August to September 2014 (2000 km northwest of Bandung) could explain why coarse-mode Zn : Al ratios drop to 0.09 for this period compared to the annual mean of 0.21.

The Bandung collocation took place in a volcanically active area, so that composition, in particular ASO$_4$, differs due to naturally variable circumstances. SPARTAN ASO$_4$ (21 %) is higher than the 4 % fraction reported by Lestari and Mauliadi (2009), but is identical with measurements by Oanh et al. (2006). SPARTAN EBC (13 %) is less than either previ-
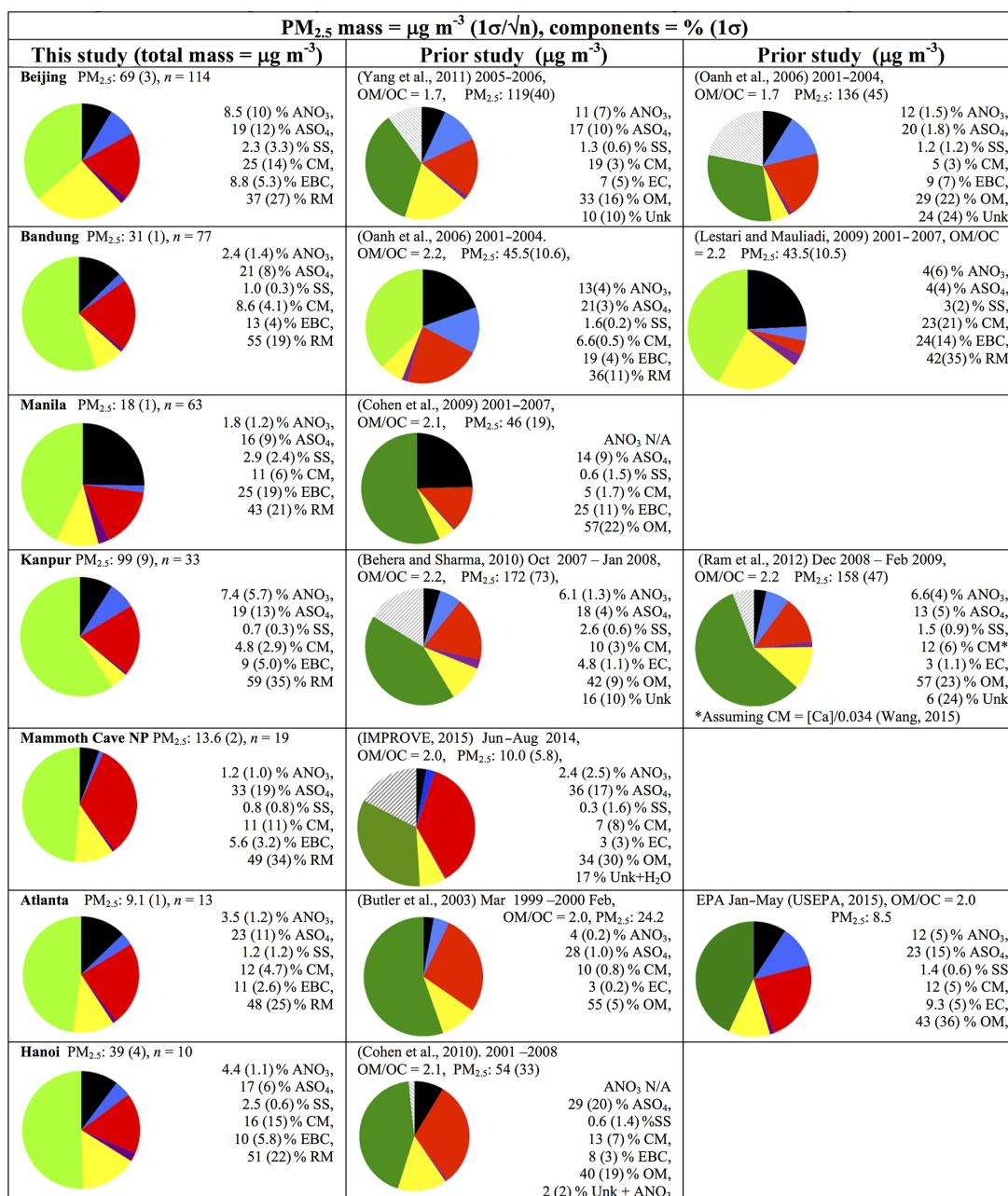
PM$_{2.5}$ mass = µg m^{-3} (1σ/√n), components = % (1σ)		
This study (total mass = µg m^{-3})	**Prior study (µg m^{-3})**	**Prior study (µg m^{-3})**
Beijing PM$_{2.5}$: 69 (3), $n = 114$ 8.5 (10) % ANO$_3$, 19 (12) % ASO$_4$, 2.3 (3.3) % SS, 25 (14) % CM, 8.8 (5.3) % EBC, 37 (27) % RM	(Yang et al., 2011) 2005–2006, OM/OC = 1.7, PM$_{2.5}$: 119(40) 11 (7) % ANO$_3$, 17 (10) % ASO$_4$, 1.3 (0.6) % SS, 19 (3) % CM, 7 (5) % EC, 33 (16) % OM, 10 (10) % Unk	(Oanh et al., 2006) 2001–2004, OM/OC = 1.7 PM$_{2.5}$: 136 (45) 12 (1.5) % ANO$_3$, 20 (1.8) % ASO$_4$, 1.2 (1.2) % SS, 5 (3) % CM, 9 (7) % EBC, 29 (22) % OM, 24 (24) % Unk
Bandung PM$_{2.5}$: 31 (1), $n = 77$ 2.4 (1.4) % ANO$_3$, 21 (8) % ASO$_4$, 1.0 (0.3) % SS, 8.6 (4.1) % CM, 13 (4) % EBC, 55 (19) % RM	(Oanh et al., 2006) 2001–2004. OM/OC = 2.2, PM$_{2.5}$: 45.5(10.6), 13(4) % ANO$_3$, 21(3) % ASO$_4$, 1.6(0.2) % SS, 6.6(0.5) % CM, 19 (4) % EBC, 36(11) % RM	(Lestari and Mauliadi, 2009) 2001–2007, OM/OC = 2.2 PM$_{2.5}$: 43.5(10.5) 4(6) % ANO$_3$, 4(4) % ASO$_4$, 3(2) % SS, 23(21) % CM, 24(14) % EBC, 42(35) % RM
Manila PM$_{2.5}$: 18 (1), $n = 63$ 1.8 (1.2) % ANO$_3$, 16 (9) % ASO$_4$, 2.9 (2.4) % SS, 11 (6) % CM, 25 (19) % EBC, 43 (21) % RM	(Cohen et al., 2009) 2001–2007, OM/OC = 2.1, PM$_{2.5}$: 46 (19), ANO$_3$ N/A 14 (9) % ASO$_4$, 0.6 (1.5) % SS, 5 (1.7) % CM, 25 (11) % EBC, 57(22) % OM,	
Kanpur PM$_{2.5}$: 99 (9), $n = 33$ 7.4 (5.7) % ANO$_3$, 19 (13) % ASO$_4$, 0.7 (0.3) % SS, 4.8 (2.9) % CM, 9 (5.0) % EBC, 59 (35) % RM	(Behera and Sharma, 2010) Oct 2007 – Jan 2008, OM/OC = 2.2, PM$_{2.5}$: 172 (73), 6.1 (1.3) % ANO$_3$, 18 (4) % ASO$_4$, 2.6 (0.6) % SS, 10 (3) % CM, 4.8 (1.1) % EC, 42 (9) % OM, 16 (10) % Unk	(Ram et al., 2012) Dec 2008 – Feb 2009, OM/OC = 2.2 PM$_{2.5}$: 158 (47) 6.6(4) % ANO$_3$, 13 (5) % ASO$_4$, 1.5 (0.9) % SS, 12 (6) % CM*, 3 (1.1) % EC, 57 (23) % OM, 6 (24) % Unk *Assuming CM = [Ca]/0.034 (Wang, 2015)
Mammoth Cave NP PM$_{2.5}$: 13.6 (2), $n = 19$ 1.2 (1.0) % ANO$_3$, 33 (19) % ASO$_4$, 0.8 (0.8) % SS, 11 (11) % CM, 5.6 (3.2) % EBC, 49 (34) % RM	(IMPROVE, 2015) Jun–Aug 2014, OM/OC = 2.0, PM$_{2.5}$: 10.0 (5.8), 2.4 (2.5) % ANO$_3$, 36 (17) % ASO$_4$, 0.3 (1.6) % SS, 7 (8) % CM, 3 (3) % EC, 34 (30) % OM, 17 % Unk+H$_2$O	
Atlanta PM$_{2.5}$: 9.1 (1), $n = 13$ 3.5 (1.2) % ANO$_3$, 23 (11) % ASO$_4$, 1.2 (1.2) % SS, 12 (4.7) % CM, 11 (2.6) % EBC, 48 (25) % RM	(Butler et al., 2003) Mar 1999 –2000 Feb, OM/OC = 2.0, PM$_{2.5}$: 24.2 4 (0.2) % ANO$_3$, 28 (1.0) % ASO$_4$, 10 (0.8) % CM, 3 (0.2) % EC, 55 (5) % OM,	EPA Jan–May (USEPA, 2015), OM/OC = 2.0 PM$_{2.5}$: 8.5 12 (5) % ANO$_3$, 23 (15) % ASO$_4$, 1.4 (0.6) % SS 12 (5) % CM, 9.3 (5) % EC, 43 (36) % OM,
Hanoi PM$_{2.5}$: 39 (4), $n = 10$ 4.4 (1.1) % ANO$_3$, 17 (6) % ASO$_4$, 2.5 (0.6) % SS, 16 (15) % CM, 10 (5.8) % EBC, 51 (22) % RM	(Cohen et al., 2010). 2001 –2008 OM/OC = 2.1, PM$_{2.5}$: 54 (33) ANO$_3$ N/A 29 (20) % ASO$_4$, 0.6 (1.4) %SS 13 (7) % CM, 8 (3) % EBC, 40 (19) % OM, 2 (2) % Unk + ANO$_3$	

Figure 3. Comparison of SPARTAN water-free aerosol composition with 11 collocated speciation studies. The numbers in parentheses show 1σ deviations of averaged masses. The number of filters sampled is n. Dark green indicates organic, light green indicates residual matter, black indicates equivalent black carbon, red indicates ammoniated sulfate, blue indicates ammonium nitrate, purple indicates sea salt, yellow indicates crustal, and grey stripes indicates what is unknown. OM : OC ratios are from Philip et al. (2014b) and Canagaratna et al. (2015). Relative mass percentages are based on water-free aerosol components. SPARTAN percentages are renormalized to 100 % after omission of species not found in comparison studies.

ous study (19 and 25 %) and the more recent analysis of 19 % BC (Santoso et al., 2013). SPARTAN ANO$_3$ is 2 %, by mass, lower than measured by Oanh et al. (2006) (13 %) but similar to Lestari and Mauliadi (2009). Both of the earlier studies show lower RM fractions (36 and 42 %) compared with 54 % RM in this study.

5.3.3 Manila, Philippines ($n = 63$)

Manila is a coastal city located in Manila Bay, adjacent to the South China Sea and surrounded by mountains. The sampling station, located at the Manila Observatory, is about 40 m higher in altitude than the central city. The PM$_{2.5}$ con-

centrations at the observatory (18 µg m^{-3}) are expected to be lower than in the main city, but still influenced by vehicular traffic, fuel combustion, and industry (Cohen et al., 2009). Compared to the all-site average, the CM fraction in Manila is typical (11 %), but equivalent black carbon is twice as great (25 %). The high EBC agrees with previous observations, attributable to a relatively high use of diesel engines (Cohen et al., 2002).

During the Manila collocation, it was found that SPARTAN fractions of ASO$_4$ and EBC are similar to Cohen et al. (2009). Our RM (43 %) is lower than OM (57 %), whereas SPARTAN CM was greater than Cohen et al. (2009). These differences could reflect sampling differences, or emission changes over the last decade.

5.3.4 Dhaka, Bangladesh ($n = 41$)

Dhaka is a densely populated city (17 000 persons km^{-2}) in a densely populated country (1100 persons km^{-2}). The sampler is situated in the heart of downtown Dhaka, on the University of Dhaka rooftop, and is influenced by air masses from the Indo-Gangetic Plain (Begum et al., 2012). More than half the country is used for agricultural purposes (Ahmed, 2014). Local contributing PM$_{2.5}$ sources include coal and biomass burning, and heavy road traffic combustion products and dust (Begum et al., 2010, 2012). PM$_{2.5}$ concentrations are the fourth-highest of any SPARTAN site, at 52 µg m^{-3}. Dhaka has the second-highest absolute EBC of any site, at 8.4 µg m^{-3}, which can be explained by the abundance of truck diesel engines (Begum et al., 2012). We estimate 41 % of PM$_{2.5}$ in Dhaka is RM. Crop or bush burning on both local and regional scales contribute significantly to organics (Begum et al., 2012). The high mean PM$_{2.5}$ Zn : Al ratio of 3.4 reflects a large contribution from urban traffic.

5.3.5 Ilorin, Nigeria ($n = 40$)

Ilorin is located in a rural area with low-level agriculture and shrub vegetation. The sampler is sited on the university campus, 15 km east of the city of 500 000 people. Aerosol loadings have seasonal cycles from agricultural burning events and dust storms (Generoso et al., 2003). The RM accounted for two-thirds of total PM$_{2.5}$ mass, among the largest, influenced by biomass burning. There is evidence of biomass burning in the PM$_{2.5}$ peak in late spring 2014, and again in 2015. Lower ASO$_4$ (12 %) compared to other SPARTAN sites reflects the sparse surrounding industry. CM levels are comparable to other locations, except during dust storms. During a dust storm (between 14 April and 2 May 2015), CM increased to two-thirds of PM$_{2.5}$ mass. The PM$_c$ Zn : Al ratio during the storm decreased to 0.01 vs. 0.25 during non-storm days.

5.3.6 Kanpur, India ($n = 33$)

Kanpur is a city of 2.5 million people. The sampler is located at the IIT Kanpur campus airstrip, about 10 km northwest of the city. The city lies in the Indo-Gangetic Plain, where massive river floodplains are used for agricultural and industrial activity (Ram et al., 2012). We sampled December 2013– May 2014, and September–November 2014, capturing one dry season. SPARTAN-measured PM$_{2.5}$ for this period was 99 µg m^{-3}, the highest of any SPARTAN site, of which 59 % is RM, 19 % ASO$_4$, and 7.4 % ANO$_3$. The absolute values of all three components are also the highest among those measured. Molar [NH$_4^+$] : [SO$_4^{2-}$] ratios are higher in Kanpur (2.6) than elsewhere. High background ammonia has been observed in the region from satellite (e.g. Clarisse et al., 2009) which could explain the high levels of ANO$_3$. Wood smoke is apparent from the high K : Al ratio (16), associated with organic matter burning during winter dry months. We detected significant Zn concentrations (Zn : Al = 1.0), which is in agreement with Misra et al. (2014) observations of a tripling of zinc during anthropogenic sourced dust.

During the Kanpur collocation, relative fractions among the major species CM, sea salt, ASO$_4$, and ANO$_3$ all matched well with previous studies (Behera and Sharma, 2010; Chakraborty et al., 2015; Ram et al., 2012) that also sampled during winter dry seasons. Chakraborty et al. (2015) measured 70 % organic mass composition and found a combined mass of 28 % for ASO$_4$+ ANO$_3$ compared to SPARTAN mass (26 %). SPARTAN ASO$_4$ (19 %) compares well to 13 % of Ram et al. (2012) and 18 % for Behera and Sharma (2010), and ANO$_3$ (7.4 %) is close to previous values (6.1 and 6.6 %). By comparison, SPARTAN slightly overestimates EBC by 4–6 %. SPARTAN CM (4.8 %) is lower than Behera and Sharma (2010) (10 %). Notably, the combined OM plus unknown fractions from these previous two studies account for almost two-thirds of aerosol mass, 58 % for Behera and Sharma (2010) and 63 % for Ram et al. (2012), similar to our 59 % RM estimate. SPARTAN PM$_{2.5}$ concentrations, as well as RM, reach a maximum during the month of December. This is consistent with recent work (Villalobos et al., 2015), who attribute this increase to agricultural burning and stagnant air.

5.3.7 Buenos Aires, Argentina ($n = 31$)

Buenos Aires has a metropolitan population of 12 million. SPARTAN instruments are located on the urban CITEDEF campus 20 km west of the central downtown. The megacity, the southernmost in our study, is surrounded by grassland and farming on the west and the Atlantic Ocean on the east. The latter explains the relatively high proportion (6 %) of sea salt. Total PM$_{2.5}$ (10 µg m^{-3}) and relative RM (31 %) are low compared with other large metropolitan areas, likely influenced by clean maritime air. In addition to sea salt and natural CM, the contribution of EBC is 17 %, which could

reflect significant local truck diesel combustion (Jasan et al., 2009).

5.3.8 Rehovot, Israel ($n = 30$)

Rehovot is located on a four-story rooftop on the Weizmann Institute campus, 11 km from the Mediterranean Sea and 20 km south of Tel Aviv. The city is surrounded by semi-arid, mixed-use cropland, and the region experiences occasional Saharan desert dust outbreaks. Typical PM$_{2.5}$ concentrations are low (16 µg m^{-3}), with the composition in Rehovot consisting of 29 % ASO$_4$, and 20 % CM. The RM fraction is smaller in Rehovot (16 % total PM$_{2.5}$ mass) than at other SPARTAN sites. Aerosol sources in Israel include agriculture, desert dust, traffic, and coal-based power plants (Graham et al., 2004). Relative sodium concentrations are high in Rehovot (4 %), similar to Buenos Aires and Ilorin, and may include a contribution from dust.

During the Lag Ba'Omer festival, we measured high ASO$_4$ concentrations on 7–18 May 2015, during which time a large number of bonfires were lit nearby. During the festival, over 75 % of total aerosol mass came from ASO$_4$ and ANO$_3$, leading to a brief doubling of the hygroscopic parameter κ_v. We observed a K : Al ratio of 38 for 6 May during the festival, the highest for any single filter.

A Saharan dust storm provided the opportunity to measure a severe dust storm in Rehovot from a filter sampling on 4–13 February 2015. The coarse filter Zn : Al ratio dropped to 0.02 during the Saharan dust storm from the typical value of 0.3. On the coarse filter, we obtained an absolute CM mass of 950 µg, which accounts for half of the collected mass during the storm. A total of 13 % of dust storm PM$_c$ is combined sea salt, ANO$_3$, and ASO$_4$, leaving 35 % RM. Although this RM fraction may imply an incomplete CM extraction, it is possible that a significant portion of desert dust carries adsorbed organic material (Falkovich et al., 2004).

5.3.9 Mammoth Cave National Park, US ($n = 19$)

The Mammoth Cave sampling site straddles national park (NP) mountainous terrain to the north and east, with farmland to the south and west. It is about 35 km from the closest town, Bowling Green, KY, with about 50 000 residents. Sources of PM are expected to be non-local, hence we consider it our background site.

For Mammoth Cave National Park collocation, this temporary SPARTAN site was deployed for comparison with the IMPROVE network station (IMPROVE, 2015). Unique among our sites, sampling was temporally coincident with IMPROVE's 1-in-3 day regimen. We obtained quality-controlled samples from June–August 2014. Temporal variation in daily values is consistent with IMPROVE for sulfate ($r^2 = 0.86$, slope $= 1.03$) and total mass of PM$_{2.5}$ ($r^2 = 0.76$, slope $= 1.12$). Differences between IMPROVE vs. SPARTAN are small for ASO$_4$ (36 % vs. 33 %), ANO$_3$ (2.4 % vs.

1.2 %), CM (7 % vs. 11 %), and EBC (3.0 % vs. 5.6 %), respectively. The combined OM, unknown, and water fraction IMPROVE was 51 %, similar to the SPARTAN RM mass fraction of 49 %.

5.3.10 Atlanta, US ($n = 13$)

Atlanta represents a major urban area in a developed country. The temporary SPARTAN site was located at the South Dekalb supersite 15 km east of downtown Atlanta. Air sampling was performed for a 4-month period spanning winter to spring 2014. Over the past 10 years, significant decreases in PM$_{2.5}$ have been observed here and across the eastern United States (Boys et al., 2014). The surrounding region is tree-covered or agricultural.

During the Atlanta (South Dekalb) collocation, co-sampled filters from the Atlanta CSN station (USEPA, 2015) provided a comparison with the summer 2014 SPARTAN data. The EPA OM fraction (43 %) agrees well with the SPARTAN mean RM (48 %). Crustal, SS, EBC, and ASO$_4$ are within 2 % relative to total composition. SPARTAN component fractions in Atlanta are also consistent with respect to Butler et al. (2003); components CM (12 % vs. 10 %), ASO$_4$ (23 % vs. 28 %), ANO$_3$ (3.5 % vs. 4 %), and RM and OM (48 % vs. 55 %) closely match, except for EBC (11 % vs. 3 %), perhaps reflecting different time periods.

5.3.11 Singapore, Singapore ($n = 12$)

Singapore is a densely populated coastal city-state of 7770 people km^{-2}. The sampler is located on a rooftop at the National University of Singapore (NUS), near the centre of the city. Transportation is of mixed use, including taxis, rail, and bicycles, which may help explain the relatively low EBC and CM of 3 %. Despite this, the Zn : Al ratio remains high at 1.5, implying a dominant traffic-based contribution to CM. SPARTAN instruments have observed significant biomass burning downwind from Indonesia, causing an increase in absolute PM$_{2.5}$ from 32 in August to 120 µg m^{-3} in September 2015, as well as an increase in RM from 44 to 62 %. The K : Al ratio steadily increased during this same period, from 7.2 (24 July–2 August 2015) to 17–24 (11 August–25 September).

5.3.12 Hanoi, Vietnam ($n = 10$)

Hanoi is an inland megacity surrounded by grassland and agriculture. The sampler itself is on a building rooftop at the Vietnam Academy of Science and Technology, 5 km northwest of the city centre. Motorbikes are the main forms of transportation downtown and the primary source of mobile-based PM$_{2.5}$ (Vu Van et al., 2013). In Hanoi, the PM$_{2.5}$ Zn : Al ratio was 3.7, also the highest of any SPARTAN site, indicative of significant traffic and tire wear.

For the Hanoi comparison SPARTAN PM$_{2.5}$ composition was generally consistent with Cohen et al. (2010). Slight

differences are perhaps related to differences in sampling season and location. SPARTAN sea salt fraction was larger (2.5 % vs. 0.6 %), but with a lower ASO$_4$ fraction (17 %) compared with Cohen et al. (2010) (29 %). Sulfate tends to be lower in the spring–summer seasons, coinciding with our measurement period, which may explain the discrepancy. SPARTAN EBC (10 %) is close to the Cohen et al. (2010) value of 8 %, whereas SPARTAN RM (51 %) and CM (16 %) masses are slightly higher.

5.3.13 Pretoria, South Africa ($n = 5$)

Pretoria is a high-altitude city (1300 m) surrounded by arid, low-intensity agriculture and extensive grasslands. The SPARTAN sampler is located on a 10 m CSIR building rooftop 12 km east of downtown area (population 700 000). Preliminary measurements of the Southern Hemisphere springtime show absolute PM$_{2.5}$ concentrations to be low, at 6.4 µg m^{-3}. There are significant fractions of CM (22 %) and EBC (22 %), and low RM (14 %). The PM$_{2.5}$ Zn : Al ratio (0.69) indicates vehicle traffic contributes to CM.

6 Refining estimates of dry hourly PM$_{2.5}$ using κ_v

Our assessment of PM$_{2.5}$ hygroscopicity is determined by site-specific chemical composition. We then use the time-varying hygroscopicity to refine the PM$_{2.5}$ values inferred from nephelometer scatter.

6.1 Relating PM$_{2.5}$ composition to κ_v

The outer pie charts of Fig. 2 show the site mean hygroscopic growth constant κ_v, surrounded by the water contributions at 35 % RH. The major contributors to PBW are ASO$_4$, ANO$_3$, RM, and sea salt, as inferred from the values listed in Table 2 and weighted by composition as in Eq. (5). ASO$_4$ and RM contribute similarly to total aerosol water, whereas ANO$_3$ contributes less to PM$_{2.5}$ hygroscopicity due to its smaller mass. The contribution of sea salt to hygroscopicity can be significant, and makes a dominant contribution in both Rehovot and Buenos Aires.

The parameter κ_v, when averaged across all sites, is 0.20, matching the generic estimate $\kappa_{v,tot} = 0.2$ applied in the initial SPARTAN study (Snider et al., 2015). Recently Brock et al. (2016) estimate κ_v values between 0.15 and 0.25 for ambient aerosols with 50 % organic composition at sub-saturated humidity. The local SPARTAN value in Atlanta (0.17) is consistent with the value of 0.16 ± 0.07 by Padró et al. (2012) in Atlanta. We found significant long-term differences in $\kappa_{v,tot}$ between cities, from 0.15 in Ilorin to 0.28 in Rehovot, and differences between filters at single sites ($\sigma \sim 0.05$). There is little correlation of $\kappa_{v,tot}$ with changes in mass ($r^2 = 0.01$). However, there are significant changes in $\kappa_{v,tot}$ due to seasonality and specific events (e.g. dust storms, fires). In Beijing, aerosol hygroscopicity was 50 % higher in mid-summer

(August) due to increased sulfate, and in late winter (March) due to a relative increase in sea salt. A summertime sulfate peak also agrees with observations by Yang et al. (2011). Table 3 shows the site-specific PBW in PM$_{2.5}$. At RH = 35 %, PBW ranges from 0.6–6 µg m^{-3}, comparable in absolute values to EBC. Above 80 % RH PBW will account for more than half of aerosol mass. Accounting for this water component in nephelometer scatter motivates the following section.

6.2 Relating nephelometer scatter to dry (RH = 35 %) PM$_{2.5}$

We apply a temporally resolved, site-specific κ_v to refine our relationship between total nephelometer scatter and PM$_{2.5}$. We calculate a 45-day running mean aerosol volume-weighted κ_v at each SPARTAN site. We then use the hygroscopic growth factors to estimate dry hourly PM$_{2.5}$ from hourly nephelometer measurements of ambient scatter and hourly measured RH. Appendix A2 describes the procedure in more detail.

We compared our hourly PM$_{2.5}$ in Beijing with PM$_{2.5}$ measurements from a beta attenuation monitor (BAM, MetOne) at the US embassy, located 15 km away. The BAM instrument contains a drying column with a 35 % humidity set point. The left panel of Fig. 4 shows the time series of hourly dry PM$_{2.5}$ concentrations predicted by SPARTAN during the summer. Pronounced temporal variation is apparent, with PM$_{2.5}$ concentrations varying by more than an order of magnitude. A high degree of consistency is found with the BAM ($r^2 = 0.67$). The exclusion of water uptake in hourly PM$_{2.5}$ estimates (by setting all κ_v to 0) decreased hourly correlations slightly to $r^2 = 0.62$. The average humidity in Beijing was 47 % for the measurement period, corresponding to a mean 17 % volume contribution by water ($\kappa_v = 0.19$). Hygroscopic growth should play a more significant role under more humid conditions (e.g. Manila and Dhaka).

The right panel in Fig. 4 shows daily-averaged PM$_{2.5}$ ($n = 148$). In 2014, there were 3167 coincidentally available hours with which to compare. The coefficient of variation for averaged 24 h measurements remained high ($r^2 = 0.70$). There was a mean offset of 10 µg m^{-3}. However, the slope is near unity (0.98), suggesting excellent proportionality between our nephelometer and the BAM instrument for PM$_{2.5}$ concentrations below 200 µg m^{-3}. Above this concentration, nephelometer signals become non-linear. The agreement remained similar for hourly values ($r^2 = 0.67$).

7 Conclusions

We have established a multi-country network where continuous monitoring with a three-wavelength nephelometer is combined with a single multi-day composite filter sample to provide information on PM$_{2.5}$. Long-term average aerosol composition is inferred from the filters, including equivalent
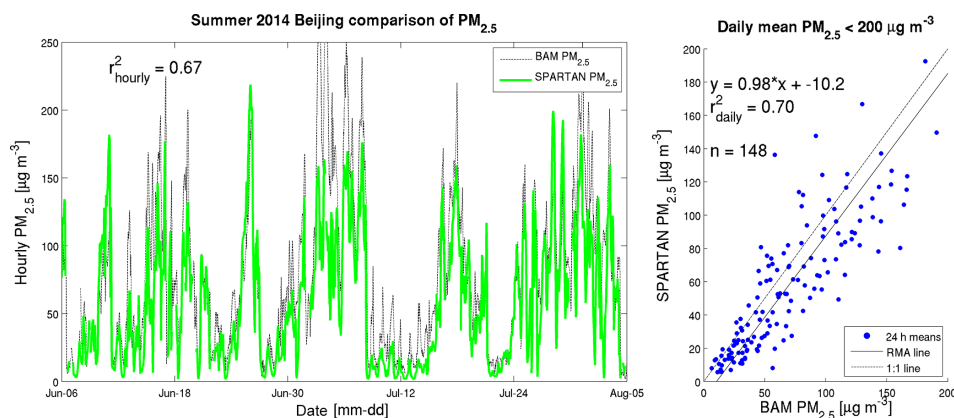
Figure 4. Left: hourly PM$_{2.5}$ estimated from SPARTAN overlaid with a MetOne BAM-1020 (June–August 2014) at the Beijing US embassy (15 km away). Right: 24 h SPARTAN PM$_{2.5}$ compared with BAM for the year 2014. Reduced major axis (RMA) slope and Pearson correlations for PM$_{2.5}$ are given in inset.

black carbon, sea salt, crustal material, ammoniated sulfate, and ammonium nitrate. This composition information was applied to calculate aerosol hygroscopicity, and in turn the relation between aerosol scatter at ambient and controlled RH. These data provide a consistent set of compositional measurements from 13 sites in 11 countries.

We report ongoing measurements of fine particulate matter (PM$_{2.5}$), including compositional information, in 13 locations in 2-month intervals or greater all within a 3-year span (2013–2016). The mean composition averaged for all SPARTAN sites is ammoniated sulfate ($20\% \pm 11\%$), crustal material ($13.4\% \pm 9.9\%$), equivalent black carbon ($11.9\% \pm 8.4\%$), ammonium nitrate ($4.7\% \pm 3.0\%$), sea salt ($2.3\% \pm 1.6\%$), trace element oxides ($1.0\% \pm 1.1\%$), water ($7.2\% \pm 3.3\%$) at 35% RH, and residual matter, which is probably primarily organic ($40\% \pm 24\%$).

Analysis of filter samples reveals that several PM$_{2.5}$ chemical components varied by more than an order of magnitude between sites. Ammoniated sulfate ranged from 1 µg m^{-3} in Buenos Aires to 17 µg m^{-3} in Kanpur (dry season). Ammonium nitrate ranged from 0.2 µg m^{-3} (Mammoth Cave, summertime) to 6.8 µg m^{-3} (Kanpur, dry season). Equivalent black carbon ranged from 0.7 µg m^{-3} (Mammoth Cave) to 8 µg m^{-3} (Dhaka and Kanpur). Locations with enhanced sulfate tend to have enhancements in other PM components. For example, ammoniated sulfate and residual matter (probably organic) are highly correlated across sites ($r^2 = 0.92$).

Crustal material concentrations ranged from 1 µg m^{-3} (Atlanta) to 16 µg m^{-3} (Beijing). Measuring Zn : Al ratios in PM$_{2.5}$ was an effective way to determine anthropogenic contribution to crustal material. Ratios larger than 0.5 identified sites with significant road dust contributions (e.g. in Hanoi, Dhaka, Manila, and Kanpur). Some locations, such as Beijing and Buenos Aires, had both high anthropogenic and natural crustal material. Low coarse Zn : Al ratios were apparent during natural dust storms. Anthropogenic crustal material is

an aerosol component neglected by most global models and which may deserve more attention.

Potassium is a known marker for wood smoke. Enhanced K : Al ratios were found in Singapore downwind of Indonesian forest fires, in Kanpur during the winter dry season from agricultural burning, and in Rehovot during a bonfire festival. Furthermore, these ratios were correlated with RM concentrations ($r^2 = 0.73$), supporting the attribution of RM as mostly organic.

SPARTAN measurements generally agree well with previous collocated studies. SPARTAN sulfate fractions are within 4% of fractions measured at 8 of the 10 collocated, though temporally non-coincident, studies. Dedicated contemporaneous collocation with IMPROVE at Mammoth Cave yielded a high degree of consistency with daily sulfate ($r^2 = 0.86$, slope = 1.03), daily PM$_{2.5}$ ($r^2 = 0.76$, slope = 1.12), and mean fractions for all major PM$_{2.5}$ components within 2%. Crustal material is typically consistent with the previous measurements, at 5–15% composition. SPARTAN equivalent black carbon ranged broadly, from 3% (Singapore) to 25% (Manila), and matched within a few percent of most previous works. Ammonium nitrate (4%) generally matched other sites, though it was sometimes lower, as in Beijing and Atlanta. Sea salt was consistently low, as found in previous measurements. Sea salt fractions were highest in Buenos Aires and Rehovot (6%), reflecting natural coastal aerosols. SPARTAN residual matter is consistent with the combined organic and unknown masses. Comparing with collocated measurements supports the expectation that most of the RM is partially organic. Residual matter could also include unaccounted-for particle-bound water, measurement error, and possibly unmeasured inorganic materials.

We calculated the hygroscopic constant κ_v for individual PM$_{2.5}$ filters to estimate water at variable humidity, and to infer wet and water-free residual matter. Based on a range of literature, we treated residual matter as mostly organic,

with constant $\kappa_{v,RM} = 0.1$. Residual matter and ammoniated sulfate largely determined overall water uptake in aerosols. These individual species, along with sea salt and ammonium nitrate, resulted in a mean mixed hygroscopic constant of 0.20, implying that for many sites, water content above 80 % RH will account for more than half of aerosol mass. For cleanroom conditions of low humidity (35 % RH), mean water composition was estimated to be 7 % by mass.

Water retention calculations allow for volumetric fluctuation estimates of aerosol water at variable RH. We subtracted the water component to predict dry nephelometer scatter as a function of time, anchored to filter masses at 35 % RH. For Beijing, we assessed the consistency of SPARTAN predictions of hourly PM$_{2.5}$ values with BAM measurements taken 15 km away, and found temporal consistency ($r^2 = 0.67$), with a slope near unity (0.98). The explained variance decreased to $r^2 = 0.62$ when setting $\kappa_v = 0$. This comparison tested both SPARTAN instrumentation and our treatment of aerosol water uptake.

These measurements provide chemical and physical data for future research on PM$_{2.5}$. Collocation with sun photometer measurements of AOD connects satellite observations to ground-based measurements and provides information needed to evaluate chemical transport model simulations of the PM$_{2.5}$ to AOD ratio. As sampling expands, SPARTAN will provide long-term data on fine aerosol variability from around the world. Ongoing work includes an analysis of trace metal concentrations and interpreting SPARTAN measurements with a chemical transport model. The data are freely available as a public good at www.spartan-network.org. We welcome expressions of interest to join this grass-roots network.

8 Data availability

SPARTAN aerosol mass and composition data are freely available at www.spartan-network.org. Hourly PM$_{2.5}$ data from Beijing is provided by the U.S. Department of State Air Quality Monitoring Program. State Air data are not fully validated and is used here only for comparative purposes with SPARTAN. Hourly PM$_{2.5}$ data from the U.S. Embassy in Beijing is provided by the U.S. Department of State Air Quality Monitoring Program. State Air PM$_{2.5}$ data is not fully validated, and used solely for comparative purposes http://www.stateair.net/web/mission/1/.

Appendix A:

A1   Estimates of organic aerosol hygroscopicity

Table A1. Hygroscopicity parameter κ_v for various studies on organic material.

κ_v (OM)	Comments	Reference
0.045	Fitted to an aged organic mixture, sub-saturated	Varutbangkul et al. (2006)
0	IMPROVE network, sub-saturated	Hand and Malm (2006)
0.10 ± 0.04	RH > 99 %, fitted to SOA precursors	Prenni et al. (2007)
$-0067 + 033(O : C)$	Fitted, RH > 99 %	Jimenez et al. (2009)
$029(O : C)$	RH > 99 %, $0.3 < O : C < 0.6$	Chang et al. (2010)
0.05	Best estimate from aged mixtures, sub-saturated	Dusek et al. (2011)
0.01–0.2	Field studies and smog chamber, sub-saturated	Duplissy et al. (2011)
0.16	RH > 99 %	Asa-Awuku et al. (2011)
0.05–0.13	Lab experiments, aged with H_2O_2 and light, sub-saturated	Liu et al. (2012)
0.1	RH > 99 %, $D_{dry} < 100$ nm	Padró et al. (2012)
$0.12\varepsilon^*_{WSOM}$	RH > 99 %	Lathem et al., 2013)
$-0005 + 019(O : C)$	Fitted, RH > 99 % 100 nm particles	Rickards et al. (2013)
0.03, 0.1	HDTMA measure, sub-saturated	Bezantakos et al. (2013)
0.1	Sub-saturated	Selected for this study

[*] ε_{WSOM} indicates fraction of water-soluble organic material.

A2

Dry aerosol scatter ($b_{\mathrm{sp,dry}}$) is related to relative humidity (RH) by

$$b_{\mathrm{sp,dry}} = \frac{b_{\mathrm{sp}}(\mathrm{RH})}{f_{\mathrm{v}}(\mathrm{RH})}. \tag{A1}$$

Changes in scatter are also proportional to mass (Chow et al., 2006; Wang et al., 2010) as

$$b_{\mathrm{sp,dry}} = \alpha \mathrm{PM}_{2.5,\mathrm{dry}}, \tag{A2}$$

where α (m^2 g^{-1}) is the mass scattering efficiency and a function of aerosol size distribution, effective radius, and dry composition. In this study, we treat composition, density, and size distribution as constant over each of our 9-day intermittent sampling periods so that $\alpha \approx <\alpha>_{9\mathrm{d}}$. Under this assumption the predicted mass changes in low humidity (35 % RH) are proportional to water-free aerosol scatter:

$$\mathrm{PM}_{2.5,\mathrm{dry}} = [<\mathrm{PM}_{2.5,\mathrm{dry}}>]\frac{b_{\mathrm{sp,dry}}}{<b_{\mathrm{sp,dry}}>}, \tag{A3}$$

where $<>$ indicates 9-day averages. The explicit compensation for aerosol water is then

$$[\mathrm{PM}_{2.5,\mathrm{dry}}] = \frac{<[\mathrm{PM}_{2.5,\mathrm{dry}}]>}{<b_{\mathrm{sp}}(\mathrm{RH})/f_{\mathrm{v}}\mathrm{RH}>} \cdot \frac{b_{\mathrm{sp}}(\mathrm{RH})}{f_{\mathrm{v}}(\mathrm{RH})}, \tag{A4}$$

where [] indicates concentration in µg m^{-3}. Uncertainties are a function of replicate weighing measurements (± 4 µg), flow volume (± 10 %), %RH (± 2.5), aerosol scatter (± 5 %), and κ_{v} (± 0.05).

$$\left(\frac{\delta[\mathrm{PM}_{2.5,\mathrm{h}}]}{[\mathrm{PM}_{2.5,\mathrm{h}}]}\right)^2 \approx \left(\frac{\delta\mathrm{PM}_{2.5}}{\mathrm{PM}_{2.5}}\right)^2 + \left(\frac{\delta V}{V}\right)^2$$
$$+ \left(\frac{\delta b_{\mathrm{sp}}}{b_{\mathrm{sp}}}\right)^2 + \left(\frac{\delta f_{\mathrm{v}}}{f_{\mathrm{v}}}\right)^2, \tag{A5}$$

where

$$\left(\frac{\delta f_{\mathrm{v}}}{f_{\mathrm{v}}}\right)^2 = \frac{(f_{\mathrm{v}}-1)^2}{f_{\mathrm{v}}^2}\left[\left(\frac{\delta\kappa}{\kappa}\right)^2 + \left(\frac{\delta\mathrm{RH}}{\mathrm{RH}\cdot(100-\mathrm{RH})}\right)^2\right]. \tag{A6}$$

The average relative 2σ PM$_{2.5}$ uncertainty was 26 % for dry hourly predictions, increasing with higher RH cutoffs. A cutoff of RH = 80 % has been applied to our data, above which hygroscopic uncertainties, as well as total water mass, dominate.

References

Ahmed, S.: Food and Agriculture in Bangladesh, Encycl. Food Agric. Ethics, 1–8, doi:10.1007/978-94-007-6167-4_61-2, 2014.

Asa-Awuku, A., Moore, R. H., Nenes, A., Bahreini, R., Holloway, J. S., Brock, C. A., Middlebrook, A. M., Ryerson, T. B., Jimenez, J. L., DeCarlo, P. F., Hecobian, A., Weber, R. J., Stickel, R., Tanner, D. J., and Huey, L. G.: Airborne cloud condensation nuclei measurements during the 2006 Texas Air Quality Study, J. Geophys. Res. Atmos., 116, D11201, doi:10.1029/2010JD014874, 2011.

Badger, C. L., George, I., Griffiths, P. T., Braban, C. F., Cox, R. A., and Abbatt, J. P. D.: Phase transitions and hygroscopic growth of aerosol particles containing humic acid and mixtures of humic acid and ammonium sulphate, Atmos. Chem. Phys., 6, 755–768, doi:10.5194/acp-6-755-2006, 2006.

Barnard, J. C., Volkamer, R., and Kassianov, E. I.: Estimation of the mass absorption cross section of the organic carbon component of aerosols in the Mexico City Metropolitan Area, Atmos. Chem. Phys., 8, 6665–6679, doi:10.5194/acp-8-6665-2008, 2008.

Begum, B. A., Biswas, S. K., Markwitz, A., and Hopke, P. K.: Identification of sources of fine and coarse particulate matter in Dhaka, Bangladesh, Aerosol Air Qual. Res., 10, 345–353, doi:10.4209/aaqr.2009.12.0082, 2010.

Begum, B. A., Hossain, A., Nahar, N., Markwitz, A., and Hopke, P. K.: Organic and black carbon in PM$_{2.5}$ at an urban site at Dhaka, Bangladesh, Aerosol Air Qual. Res., 12, 1062–1072, 2012.

Behera, S. N. and Sharma, M.: Reconstructing primary and secondary components of PM$_{2.5}$ composition for an urban atmosphere, Aerosol Sci. Technol., 44, 983–992, doi:10.1080/02786826.2010.504245, 2010.

Bell, M. L., Dominici, F., Ebisu, K., Zeger, S. L., and Samet, J. M.: Spatial and temporal variation in PM$_{2.5}$ chemical composition in the United States for health effects studies, Environ. Health Perspect., 115, 989–995, doi:10.2307/4619499, 2007.

Bezantakos, S., Barmpounis, K., Giamarelou, M., Bossioli, E., Tombrou, M., Mihalopoulos, N., Eleftheriadis, K., Kalogiros, J., D. Allan, J., Bacak, A., Percival, C. J., Coe, H., and Biskos, G.: Chemical composition and hygroscopic properties of aerosol particles over the Aegean Sea, Atmos. Chem. Phys., 13, 11595–11608, doi:10.5194/acp-13-11595-2013, 2013.

Bond, T. C. and Bergstrom, R. W.: Light absorption by carbonaceous particles: an investigative review, Aerosol Sci. Technol., 40, 27–67, doi:10.1080/02786820500421521, 2006.

Boys, B. L., Martin, R. V, van Donkelaar, A., MacDonell, R. J., Hsu, N. C., Cooper, M. J., Yantosca, R. M., Lu, Z., Streets, D. G., Zhang, Q., and Wang, S. W.: Fifteen-year global time series of satellite-derived fine particulate matter, Environ. Sci. Technol., 48, 11109–11118, doi:10.1021/es502113p, 2014.

Brauer, M., Freedman, G., Frostad, J., van Donkelaar, A., Martin, R. V, Dentener, F., Dingenen, R. van, Estep, K., Amini, H., Apte, J. S., Balakrishnan, K., Barregard, L., Broday, D., Feigin, V., Ghosh, S., Hopke, P. K., Knibbs, L. D., Kokubo, Y., Liu, Y., Ma, S., Morawska, L., Sangrador, J. L. T., Shaddick, G., Anderson, H. R., Vos, T., Forouzanfar, M. H., Burnett, R. T. and Cohen, A.: Ambient air pollution exposure estimation for the Global Burden of Disease 2013, Environ. Sci. Technol., 50, 79–88, doi:10.1021/acs.est.5b03709, 2015.

Brock, C. A., Wagner, N. L., Anderson, B. E., Beyersdorf, A., Campuzano-Jost, P., Day, D. A., Diskin, G. S., Gordon, T. D., Jimenez, J. L., Lack, D. A., Liao, J., Markovic, M. Z., Middlebrook, A. M., Perring, A. E., Richardson, M. S., Schwarz, J. P., Welti, A., Ziemba, L. D., and Murphy, D. M.: Aerosol optical properties in the southeastern United States in summer – Part 2: Sensitivity of aerosol optical depth to relative humidity and aerosol parameters, Atmos. Chem. Phys., 16, 5009–5019, doi:10.5194/acp-16-5009-2016, 2016.

Butler, A. J., Andrew, M. S., and Russell, A. G.: Daily sampling of PM2.5 in Atlanta: results of the first year of the assessment of spatial aerosol composition in Atlanta study, J. Geophys. Res. Atmos., 108, 8415, doi:10.1029/2002JD002234, 2003.

Canagaratna, M. R., Jimenez, J. L., Kroll, J. H., Chen, Q., Kessler, S. H., Massoli, P., Hildebrandt Ruiz, L., Fortner, E., Williams, L. R., Wilson, K. R., Surratt, J. D., Donahue, N. M., Jayne, J. T., and Worsnop, D. R.: Elemental ratio measurements of organic compounds using aerosol mass spectrometry: characterization, improved calibration, and implications, Atmos. Chem. Phys., 15, 253–272, doi:10.5194/acp-15-253-2015, 2015.

Carrico, C. M., Petters, M. D., Kreidenweis, S. M., Sullivan, A. P., McMeeking, G. R., Levin, E. J. T., Engling, G., Malm, W. C., and Collett Jr., J. L.: Water uptake and chemical composition of fresh aerosols generated in open burning of biomass, Atmos. Chem. Phys., 10, 5165–5178, doi:10.5194/acp-10-5165-2010, 2010.

Chakraborty, A., Bhattu, D., Gupta, T., Tripathi, S. N., and Canagaratna, M. R.: Real-time measurements of ambient aerosols in a polluted Indian city: Sources, characteristics, and processing of organic aerosols during foggy and nonfoggy periods, J. Geophys. Res. Atmos., 120, 2015JD023419, doi:10.1002/2015JD023419, 2015.

Chang, R. Y.-W., Slowik, J. G., Shantz, N. C., Vlasenko, A., Liggio, J., Sjostedt, S. J., Leaitch, W. R., and Abbatt, J. P. D.: The hygroscopicity parameter (κ) of ambient organic aerosol at a field

site subject to biogenic and anthropogenic influences: relationship to degree of aerosol oxidation, Atmos. Chem. Phys., 10, 5047–5064, doi:10.5194/acp-10-5047-2010, 2010.

Chen, H., Goldberg, M. S., and Villeneuve, P. J.: A systematic review of the relation between long-term exposure to ambient air pollution and chronic diseases, Rev. Environ. Health, 23, 243–297, 2008.

Chen, Z., Wang, J.-N., Ma, G.-X., and Zhang, Y.-S.: China tackles the health effects of air pollution, Lancet, 382, 1959–1960, 2013.

Chow, J. C., Watson, J. G., Park, K., Lowenthal, D. H., Robinson, N. F., and Magliano, K. A.: Comparison of particle light scattering and fine particulate matter mass in central California, J. Air Waste Manage. Assoc., 56, 398–410, 2006.

Chu, S.-H.: PM$_{2.5}$ episodes as observed in the speciation trends network, Atmos. Environ., 38, 5237–5246, doi:10.1016/j.atmosenv.2004.01.055, 2004.

Clarisse, L., Clerbaux, C., Dentener, F., Hurtmans, D., and Coheur, P.-F.: Global ammonia distribution derived from infrared satellite observations, Nat. Geosci., 2, 479–483, 2009.

Cohen, D. D., Garton, D., Stelcer, E., Wang, T., Poon, S., Kim, J., Oh, S. N., Shin, H.-J., Ko, M. Y. and Santos, F.: Characterisation of PM$_{2.5}$ and PM10 fine particle pollution in several Asian regions, 16th Int. Clear Air Conf. Christchurch, NZ, 18–22 August 2002.

Cohen, D. D., Stelcer, E., Santos, F. L., Prior, M., Thompson, C., and Pabroa, P. C. B.: Fingerprinting and source apportionment of fine particle pollution in Manila by IBA and PMF techniques: A 7-year study, X-Ray Spectrom., 38, 18–25, doi:10.1002/xrs.1112, 2009.

Cohen, D. D., Crawford, J., Stelcer, E., and Bac, V. T.: Characterisation and source apportionment of fine particulate sources at Hanoi from 2001 to 2008, Atmos. Environ., 44, 320–328, doi:10.1016/j.atmosenv.2009.10.037, 2010.

Councell, T. B., Duckenfield, K. U., Landa, E. R., and Callender, E.: Tire-wear particles as a source of zinc to the environment, Environ. Sci. Technol., 38, 4206–4214, doi:10.1021/es034631f, 2004.

Dabek-Zlotorzynska, E., Dann, T. F., Kalyani Martinelango, P., Celo, V., Brook, J. R., Mathieu, D., Ding, L., and Austin, C. C.: Canadian National Air Pollution Surveillance (NAPS) PM$_{2.5}$ speciation program: Methodology and PM$_{2.5}$ chemical composition for the years 2003–2008, Atmos. Environ., 45, 673–686, 2011.

Duplissy, J., DeCarlo, P. F., Dommen, J., Alfarra, M. R., Metzger, A., Barmpadimos, I., Prevot, A. S. H., Weingartner, E., Tritscher, T., Gysel, M., Aiken, A. C., Jimenez, J. L., Canagaratna, M. R., Worsnop, D. R., Collins, D. R., Tomlinson, J., and Baltensperger, U.: Relating hygroscopicity and composition of organic aerosol particulate matter, Atmos. Chem. Phys., 11, 1155–1165, doi:10.5194/acp-11-1155-2011, 2011.

Dusek, U., Frank, G. P., Massling, A., Zeromskiene, K., Iinuma, Y., Schmid, O., Helas, G., Hennig, T., Wiedensohler, A., and Andreae, M. O.: Water uptake by biomass burning aerosol at sub- and supersaturated conditions: closure studies and implications for the role of organics, Atmos. Chem. Phys., 11, 9519–9532, doi:10.5194/acp-11-9519-2011, 2011.

Falkovich, A. H., Schkolnik, G., Ganor, E., and Rudich, Y.: Adsorption of organic compounds pertinent to urban environments onto mineral dust particles, J. Geophys. Res. Atmos., 109, 2156–2202, doi:10.1029/2003JD003919, 2004.

Fang, T., Guo, H., Verma, V., Peltier, R. E., and Weber, R. J.: PM$_{2.5}$ water-soluble elements in the southeastern United States: automated analytical method development, spatiotemporal distributions, source apportionment, and implications for heath studies, Atmos. Chem. Phys., 15, 11667–11682, doi:10.5194/acp-15-11667-2015, 2015.

Forouzanfar, M. H., Alexander, L., Anderson, H. R., Bachman, V. F., Biryukov, S., Brauer, M., Burnett, R., Casey, D., Coates, M. M., Cohen, A., Delwiche, K., Estep, K., Frostad, J. J., KC, A., Kyu, H. H., Moradi-Lakeh, M., Ng, M., Slepak, E. L., Thomas, B. A., Wagner, J., Aasvang, G. M., Abbafati, C., Ozgoren, A. A., Abd-Allah, F., Abera, S. F., Aboyans, V., Abraham, B., Abraham, J. P., Abubakar, I., Abu-Rmeileh, N. M. E., Aburto, T. C., Achoki, T., Adelekan, A., Adofo, K., Adou, A. K., Adsuar, J. C., Afshin, A., Agardh, E. E., Al Khabouri, M. J., Al Lami, F. H., Alam, S. S., Alasfoor, D., Albittar, M. I., Alegretti, M. A., Aleman, A. V, Alemu, Z. A., Alfonso-Cristancho, R., Alhabib, S., Ali, R., Ali, M. K., Alla, F., Allebeck, P., Allen, P. J., Alsharif, U., Alvarez, E., Alvis-Guzman, N., Amankwaa, A. A., Amare, A. T., Ameh, E. A., Ameli, O., Amini, H., Ammar, W., Anderson, B. O., Antonio, C. A. T., Anwari, P., Cunningham, S. A., Arnlöv, J., Arsenijevic, V. S. A., Artaman, A., Asghar, R. J., Assadi, R., Atkins, L. S., Atkinson, C., Avila, M. A., Awuah, B., Badawi, A., Bahit, M. C., Bakfalouni, T., Balakrishnan, K., Balalla, S., Balu, R. K., Banerjee, A., Barber, R. M., Barker-Collo, S. L., Barquera, S., Barregard, L., Barrero, L. H., Barrientos-Gutierrez, T., Basto-Abreu, A. C., Basu, A., Basu, S., Basulaiman, M. O., Ruvalcaba, C. B., Beardsley, J., Bedi, N., Bekele, T., Bell, M. L., Benjet, C., Bennett, D. A., et al.: Global, regional, and national comparative risk assessment of 79 behavioural, environmental and occupational, and metabolic risks or clusters of risks in 188 countries, 1990–2013: a systematic analysis for the Global Burden of Disease Study 2013, Lancet, 386, 2287–2323, doi:10.1016/S0140-6736(15)00128-2, 2015.

Fountoukis, C. and Nenes, A.: ISORROPIA II: a computationally efficient thermodynamic equilibrium model for K$^+$–Ca^{2+}–Mg^{2+}–NH$_4^+$–Na$^+$–SO$_4^{2-}$–NO$_3^-$–Cl$^-$–H$_2$O aerosols, Atmos. Chem. Phys., 7, 4639–4659, doi:10.5194/acp-7-4639-2007, 2007.

Fujii, Y., Iriana, W., Oda, M., Puriwigati, A., Tohno, S., Lestari, P., Mizohata, A., and Huboyo, H. S.: Characteristics of carbonaceous aerosols emitted from peatland fire in Riau, Sumatra, Indonesia, Atmos. Environ., 87, 164–169, doi:10.1016/j.atmosenv.2014.01.037, 2014.

Generoso, S., Bréon, F.-M., Balkanski, Y., Boucher, O., and Schulz, M.: Improving the seasonal cycle and interannual variations of biomass burning aerosol sources, Atmos. Chem. Phys., 3, 1211–1222, doi:10.5194/acp-3-1211-2003, 2003.

Gibson, M. D., Heal, M. R., Bache, D. H., Hursthouse, A. S., Beverland, I. J., Craig, S. E., Clark, C. F., Jackson, M. H., Guernsey, J. R., and Jones, C.: Using mass reconstruction along a four-site transect as a method to interpret PM$_{10}$ in west-central Scotland, United Kingdom, J. Air Waste Manage. Assoc., 59, 1429–1436, doi:10.3155/1047-3289.59.12.1429, 2009.

Gibson, M. D., Pierce, J. R., Waugh, D., Kuchta, J. S., Chisholm, L., Duck, T. J., Hopper, J. T., Beauchamp, S., King, G. H., Franklin, J. E., Leaitch, W. R., Wheeler, A. J., Li, Z., Gagnon, G. A.,

and Palmer, P. I.: Identifying the sources driving observed PM$_{2.5}$ temporal variability over Halifax, Nova Scotia, during BORTAS-B, Atmos. Chem. Phys., 13, 7199–7213, doi:10.5194/acp-13-7199-2013, 2013a.

Gibson, M. D., Heal, M. R., Li, Z., Kuchta, J., King, G. H., Hayes, A., and Lambert, S.: The spatial and seasonal variation of nitrogen dioxide and sulfur dioxide in Cape Breton Highlands National Park, Canada, and the association with lichen abundance, Atmos. Environ., 64, 303–311, doi:10.1016/j.atmosenv.2012.09.068, 2013b.

Giordano, M. R., Short, D. Z., Hosseini, S., Lichtenberg, W., and Asa-Awuku, A. A.: Changes in droplet surface tension affect the observed hygroscopicity of photochemically aged biomass burning aerosol, Environ. Sci. Technol., 47, 10980–10986, doi:10.1021/es401867j, 2013.

Graham, B., Falkovich, A. H., Rudich, Y., Maenhaut, W., Guyon, P. and Andreae, M. O.: Local and regional contributions to the atmospheric aerosol over Tel Aviv, Israel: a case study using elemental, ionic and organic tracers, Atmos. Environ., 38, 1593–1604, doi:10.1016/j.atmosenv.2003.12.015, 2004.

Hand, J. and Malm, W. C.: Review of the IMPROVE equation for estimating ambient light extinction coefficients, Colorado State University, Fort Colins, 2006.

Hand, J. L., Schichtel, B. A., Pitchford, M., Malm, W. C., and Frank, N. H.: Seasonal composition of remote and urban fine particulate matter in the United States, J. Geophys. Res., 117, D05209, doi:10.1029/2011JD017122, 2012.

Henning, S., Weingartner, E., Schwikowski, M., Gäggeler, H. W., Gehrig, R., Hinz, K.-P., Trimborn, A., Spengler, B., and Baltensperger, U.: Seasonal variation of water-soluble ions of the aerosol at the high-alpine site Jungfraujoch (3580 m asl), J. Geophys. Res. Atmos., 108, 4030, doi:10.1029/2002JD002439, 2003.

Hersey, S. P., Craven, J. S., Metcalf, A. R., Lin, J., Lathem, T., Suski, K. J., Cahill, J. F., Duong, H. T., Sorooshian, A., Jonsson, H. H., Shiraiwa, M., Zuend, A., Nenes, A., Prather, K. A., Flagan, R. C., and Seinfeld, J. H.: Composition and hygroscopicity of the Los Angeles Aerosol: CalNex, J. Geophys. Res. Atmos., 118, 3016–3036, doi:10.1002/jgrd.50307, 2013.

Holben, B. N., Eck, T. F., Slutsker, I., Tanré, D., Buis, J. P., Setzer, A., Vermote, E., Reagan, J. A., Kaufman, Y. J., Nakajima, T., Lavenu, F., Jankowiak, I., and Smirnov, A.: AERONET—A federated instrument network and data archive for aerosol characterization, Remote Sens. Environ., 66, 1–16, doi:10.1016/S0034-4257(98)00031-5, 1998.

Huang, J. P., Liu, J. J., Chen, B., and Nasiri, S. L.: Detection of anthropogenic dust using CALIPSO lidar measurements, Atmos. Chem. Phys., 15, 11653–11665, doi:10.5194/acp-15-11653-2015, 2015.

IMPROVE: Reconstructing Light Extinction from Aerosol Measurements, Reconstr. Light Extinction from Aerosol Meas. Interag. Monit. Prot. Vis. Environ, availabe at: http://views.cira.colostate.edu/fed/DataWizard/Default.aspx (last access: 22 July 2016), 2015.

IPCC: Climate Change 2013: The Physical Science Basis. Contribution of Working Group I to the Fifth Assessment Report of the Intergovernmental Panel on Climate Change, 5th Edn., edited by: Stocker, T. F., Qin, D., Plattner, G.-K., Tignor, M., Allen, S. K., Boschung, J., Nauels, A., Xia, Y., Bex, V., and Midgley, P. M.,

Cambridge University Press, Cambridge, United Kingdom and New York, NY, USA, 2013.

Jasan, R. C., Plá, R. R., Invernizzi, R., and Dos Santos, M.: Characterization of atmospheric aerosol in Buenos Aires, Argentina, J. Radioanal. Nucl. Chem., 281, 101–105, doi:10.1007/s10967-009-0071-1, 2009.

Jimenez, J. L., Canagaratna, M. R., Donahue, N. M., Prevot, A. S. H., Zhang, Q., Kroll, J. H., DeCarlo, P. F., Allan, J. D., Coe, H., Ng, N. L., Aiken, A. C., Docherty, K. S., Ulbrich, I. M., Grieshop, A. P., Robinson, A. L., Duplissy, J., Smith, J. D., Wilson, K. R., Lanz, V. A., Hueglin, C., Sun, Y. L., Tian, J., Laaksonen, A., Raatikainen, T., Rautiainen, J., Vaattovaara, P., Ehn, M., Kulmala, M., Tomlinson, J. M., Collins, D. R., Cubison, M. J., E., Dunlea, J., Huffman, J. A., Onasch, T. B., Alfarra, M. R., Williams, P. I., Bower, K., Kondo, Y., Schneider, J., Drewnick, F., Borrmann, S., Weimer, S., Demerjian, K., Salcedo, D., Cottrell, L., Griffin, R., Takami, A., Miyoshi, T., Hatakeyama, S., Shimono, A., Sun, J. Y., Zhang, Y. M., Dzepina, K., Kimmel, J. R., Sueper, D., Jayne, J. T., Herndon, S. C., Trimborn, A. M., Williams, L. R., Wood, E. C., Middlebrook, A. M., Kolb, C. E., Baltensperger, U., and Worsnop, D. R.: Evolution of organic aerosols in the atmosphere, Science, 326, 1525–1529, doi:10.1126/science.1180353, 2009.

Kahn, R. A. and Gaitley, B. J.: An analysis of global aerosol type as retrieved by MISR, J. Geophys. Res. Atmos., 120, 4248–4281, doi:10.1002/2015JD023322, 2015.

Kloog, I., Koutrakis, P., Coull, B. A., Lee, H. J., and Schwartz, J.: Assessing temporally and spatially resolved PM$_{2.5}$ exposures for epidemiological studies using satellite aerosol optical depth measurements, Atmos. Environ., 45, 6267–6275, doi:10.1016/j.atmosenv.2011.08.066, 2011.

Kloog, I., Ridgway, B., Koutrakis, P., Coull, B. A., and Schwartz, J. D.: Long- and short-term exposure to PM(2.5) and mortality: Using novel exposure models, Epidemiology, 24, 555–561, doi:10.1097/EDE.0b013e318294beaa, 2013.

Koepke, P., Hess, M., Schult, I., and Shettle, E. P.: Global Aerosol Dataset, Report N 243, Hamburg, 1997.

Kreidenweis, S. M., Petters, M. D., and DeMott, P. J.: Single-parameter estimates of aerosol water content, Environ. Res. Lett., 3, 35002, doi:10.1088/1748-9326/3/3/035002, 2008.

Laden, F., Schwartz, J., Speizer, F. E., and Dockery, D. W.: Reduction in fine particulate air pollution and mortality, Am. J. Respir. Crit. Care Med., 173, 667–672, doi:10.1164/rccm.200503-443OC, 2006.

Latham, J., Cumani, R., Rosati, I., and Bloise, M.: Global Land Cover SHARE (GLC-SHARE) database Beta-Release Version 1.0-2014, Rome, 2014.

Lathem, T. L., Beyersdorf, A. J., Thornhill, K. L., Winstead, E. L., Cubison, M. J., Hecobian, A., Jimenez, J. L., Weber, R. J., Anderson, B. E., and Nenes, A.: Analysis of CCN activity of Arctic aerosol and Canadian biomass burning during summer 2008, Atmos. Chem. Phys., 13, 2735–2756, doi:10.5194/acp-13-2735-2013, 2013.

Lee, H. J., Coull, B. A., Bell, M. L., and Koutrakis, P.: Use of satellite-based aerosol optical depth and spatial clustering to predict ambient PM$_{2.5}$ concentrations, Environ. Res., 118, 8–15, doi:10.1016/j.envres.2012.06.011, 2012.

Lelieveld, J., Evans, J. S., Fnais, M., Giannadaki, D. and Pozzer, A.: The contribution of outdoor air pollution sources to premature mortality on a global scale, Nature, 525(7569), 367–371, 2015.

Lepeule, J., Laden, F., Dockery, D., and Schwartz, J.: Chronic Exposure to Fine Particles and Mortality: An Extended Follow-up of the Harvard Six Cities Study from 1974 to 2009, Environ. Health Perspect., 120, 965–970, doi:10.1289/ehp.1104660, 2012.

Lestari, P. and Mauliadi, Y. D.: Source apportionment of particulate matter at urban mixed site in Indonesia using PMF, Atmos. Environ., 43, 1760–1770, doi:10.1016/j.atmosenv.2008.12.044, 2009.

Lin, C., Li, Y., Yuan, Z., Lau, A. K. H., Li, C., and Fung, J. C. H.: Using satellite remote sensing data to estimate the high-resolution distribution of ground-level PM$_{2.5}$, Remote Sens. Environ., 156, 117–128, doi:10.1016/j.rse.2014.09.015, 2015.

Lippmann, M.: Toxicological and epidemiological studies of cardiovascular effects of ambient air fine particulate matter (PM$_{2.5}$) and its chemical components: Coherence and public health implications, Crit. Rev. Toxicol., 44, 299–347, doi:10.3109/10408444.2013.861796, 2014.

Liu, Y., Monod, A., Tritscher, T., Praplan, A. P., DeCarlo, P. F., Temime-Roussel, B., Quivet, E., Marchand, N., Dommen, J., and Baltensperger, U.: Aqueous phase processing of secondary organic aerosol from isoprene photooxidation, Atmos. Chem. Phys., 12, 5879–5895, doi:10.5194/acp-12-5879-2012, 2012.

Malm, W. C., Sisler, J. F., Huffman, D., Eldred, R. A., and Cahill, T. A.: Spatial and seasonal trends in particle concentration and optical extinction in the United States, J. Geophys. Res., 99, 1347–1370, 1994.

Misra, A., Gaur, A., Bhattu, D., Ghosh, S., Dwivedi, A. K., Dalai, R., Paul, D., Gupta, T., Tare, V., Mishra, S. K., Singh, S., and Tripathi, S. N.: An overview of the physico-chemical characteristics of dust at Kanpur in the central Indo-Gangetic basin, Atmos. Environ., 97, 386–396, doi:10.1016/j.atmosenv.2014.08.043, 2014.

Munchak, L. A., Schichtel, B. A., Sullivan, A. P., Holden, A. S., Kreidenweis, S. M., Malm, W. C., and Collett, J. L.: Development of wildland fire particulate smoke marker to organic carbon emission ratios for the conterminous United States, Atmos. Environ., 45, 395–403, doi:10.1016/j.atmosenv.2010.10.006, 2011.

Oanh, N. T. K., Upadhyay, N., Zhuang, Y.-H., Hao, Z.-P., Murthy, D. V. S., Lestari, P., Villarin, J. T., Chengchua, K., Co, H. X., Dung, N. T., and Lindgren, E. S.: Particulate air pollution in six Asian cities: Spatial and temporal distributions, and associated sources, Atmos. Environ., 40, 3367–3380, doi:10.1016/j.atmosenv.2006.01.050, 2006.

Padró, L. T., Moore, R. H., Zhang, X., Rastogi, N., Weber, R. J., and Nenes, A.: Mixing state and compositional effects on CCN activity and droplet growth kinetics of size-resolved CCN in an urban environment, Atmos. Chem. Phys., 12, 10239–10255, doi:10.5194/acp-12-10239-2012, 2012.

Patadia, F., Kahn, R. A., Limbacher, J. A., Burton, S. P., Ferrare, R. A., Hostetler, C. A., and Hair, J. W.: Aerosol airmass type mapping over the Urban Mexico City region from space-based multi-angle imaging, Atmos. Chem. Phys., 13, 9525–9541, doi:10.5194/acp-13-9525-2013, 2013.

Petters, M. D. and Kreidenweis, S. M.: A single parameter representation of hygroscopic growth and cloud condensation nucleus activity, Atmos. Chem. Phys., 7, 1961–1971, doi:10.5194/acp-7-1961-2007, 2007.

Petters, M. D. and Kreidenweis, S. M.: A single parameter representation of hygroscopic growth and cloud condensation nucleus activity – Part 2: Including solubility, Atmos. Chem. Phys., 8, 6273–6279, doi:10.5194/acp-8-6273-2008, 2008.

Petters, M. D. and Kreidenweis, S. M.: A single parameter representation of hygroscopic growth and cloud condensation nucleus activity – Part 3: Including surfactant partitioning, Atmos. Chem. Phys., 13, 1081–1091, doi:10.5194/acp-13-1081-2013, 2013.

Petzold, A., Ogren, J. A., Fiebig, M., Laj, P., Li, S.-M., Baltensperger, U., Holzer-Popp, T., Kinne, S., Pappalardo, G., Sugimoto, N., Wehrli, C., Wiedensohler, A., and Zhang, X.-Y.: Recommendations for reporting "black carbon" measurements, Atmos. Chem. Phys., 13, 8365–8379, doi:10.5194/acp-13-8365-2013, 2013.

Philip, S., Martin, R. V, van Donkelaar, A., Lo, J. W.-H., Wang, Y., Chen, D., Zhang, L., Kasibhatla, P. S., Wang, S., Zhang, Q., Lu, Z., Streets, D. G., Bittman, S., and Macdonald, D. J.: Global chemical composition of ambient fine particulate matter for exposure assessment, Environ. Sci. Technol., 48, 13060–13068, doi:10.1021/es502965b, 2014a.

Philip, S., Martin, R. V., Pierce, J. R., Jimenez, J. L., Zhang, Q., Canagaratna, M. R., Spracklen, D. V., Nowlan, C. R., Lamsal, L. N., Cooper, M. J., and Krotkov, N. A.: Spatially and seasonally resolved estimate of the ratio of organic mass to organic carbon, Atmos. Environ., 87, 34–40, doi:10.1016/j.atmosenv.2013.11.065, 2014b.

Pitchford, M., Malm, W., Schichtel, B., Kumar, N., Lowenthal, D., and Hand, J.: Revised algorithm for estimating light extinction from IMPROVE particle speciation data, J. Air Waste Manage. Assoc., 57, 1326–1336, doi:10.3155/1047-3289.57.11.1326, 2007.

Prenni, A. J., Petters, M. D., Kreidenweis, S. M., DeMott, P. J., and Ziemann, P. J.: Cloud droplet activation of secondary organic aerosol, J. Geophys. Res., 112, D10223, doi:10.1029/2006JD007963, 2007.

Putaud, J.-P., Raes, F., Van Dingenen, R., Brüggemann, E., Facchini, M.-C., Decesari, S., Fuzzi, S., Gehrig, R., Hüglin, C., Laj, P., Lorbeer, G., Maenhaut, W., Mihalopoulos, N., Müller, K., Querol, X., Rodriguez, S., Schneider, J., Spindler, G., Brink, H. ten, Tørseth, K., and Wiedensohler, A.: A European aerosol phenomenology—2: chemical characteristics of particulate matter at kerbside, urban, rural and background sites in Europe, Atmos. Environ., 38, 2579–2595, doi:10.1016/j.atmosenv.2004.01.041, 2004.

Putaud, J.-P., Van Dingenen, R., Alastuey, A., Bauer, H., Birmili, W., Cyrys, J., Flentje, H., Fuzzi, S., Gehrig, R., Hansson, H. C., Harrison, R. M., Herrmann, H., Hitzenberger, R., Hüglin, C., Jones, A. M., Kasper-Giebl, A., Kiss, G., Kousa, A., Kuhlbusch, T. A. J., Löschau, G., Maenhaut, W., Molnar, A., Moreno, T., Pekkanen, J., Perrino, C., Pitz, M., Puxbaum, H., Querol, X., Rodriguez, S., Salma, I., Schwarz, J., Smolik, J., Schneider, J., Spindler, G., ten Brink, H., Tursic, J., Viana, M., Wiedensohler, A., and Raes, F.: A European aerosol phenomenology – 3: Physical and chemical characteristics of particulate matter from 60 rural, urban, and kerbside sites across Europe, Atmos. Environ., 44, 1308–1320, doi:10.1016/j.atmosenv.2009.12.011, 2010.

Quincey, P., Butterfield, D., Green, D., Coyle, M., and Cape, J. N.: An evaluation of measurement methods for organic, elemental

and black carbon in ambient air monitoring sites, Atmos. Environ., 43, 5085–5091, doi:10.1016/j.atmosenv.2009.06.041, 2009.

Ram, K., Sarin, M. M., and Tripathi, S. N.: Temporal trends in atmospheric PM$_{2.5}$, PM$_{10}$, elemental carbon, organic carbon, water-soluble organic carbon, and optical properties: Impact of biomass burning emissions in the Indo-Gangetic Plain, Environ. Sci. Technol., 46, 686–695, doi:10.1021/es202857w, 2012.

Remoundaki, E., Kassomenos, P., Mantas, E., Mihalopoulos, N., and Tsezos, M.: Composition and mass closure of PM$_{2.5}$ in urban environment (Athens, Greece), Aerosol Air Qual. Res., 13, 72–82, 2013.

Rice, E. W., Bridgewater, L., Association, A. P. H., Association, A. W. W., and Federation, W. E.: Standard Methods for the Examination of Water and Wastewater, American Public Health Association, 2012.

Rickards, A. M. J., Miles, R. E. H., Davies, J. F., Marshall, F. H., and Reid, J. P.: Measurements of the sensitivity of aerosol hygroscopicity and the κ parameter to the O/C ratio, J. Phys. Chem. A, 117, 14120–14131, doi:10.1021/jp407991n, 2013.

Robinson, C. B., Schill, G. P., Zarzana, K. J., and Tolbert, M. A.: Impact of organic coating on optical growth of ammonium sulfate particles, Environ. Sci. Technol., 47, 13339–13346, doi:10.1021/es4023128, 2013.

Santoso, M., Dwiana Lestiani, D., and Hopke, P. K.: Atmospheric black carbon in PM$_{2.5}$ in Indonesian cities, J. Air Waste Manage. Assoc., 63, 1022–1025, doi:10.1080/10962247.2013.804465, 2013.

Snider, G., Weagle, C. L., Martin, R. V., van Donkelaar, A., Conrad, K., Cunningham, D., Gordon, C., Zwicker, M., Akoshile, C., Artaxo, P., Anh, N. X., Brook, J., Dong, J., Garland, R. M., Greenwald, R., Griffith, D., He, K., Holben, B. N., Kahn, R., Koren, I., Lagrosas, N., Lestari, P., Ma, Z., Vanderlei Martins, J., Quel, E. J., Rudich, Y., Salam, A., Tripathi, S. N., Yu, C., Zhang, Q., Zhang, Y., Brauer, M., Cohen, A., Gibson, M. D., and Liu, Y.: SPARTAN: a global network to evaluate and enhance satellite-based estimates of ground-level particulate matter for global health applications, Atmos. Meas. Tech., 8, 505–521, doi:10.5194/amt-8-505-2015, 2015.

Sorooshian, A., Hersey, S., Brechtel, F. J., Corless, A., Flagan, R. C., and Seinfeld, J. H.: Rapid, size-resolved aerosol hygroscopic growth measurements: differential aerosol sizing and hygroscopicity spectrometer probe (DASH-SP), Aerosol Sci. Technol., 42, 445–464, doi:10.1080/02786820802178506, 2008.

Sun, Y.-L., Zhang, Q., Schwab, J. J., Demerjian, K. L., Chen, W.-N., Bae, M.-S., Hung, H.-M., Hogrefe, O., Frank, B., Rattigan, O. V., and Lin, Y.-C.: Characterization of the sources and processes of organic and inorganic aerosols in New York city with a high-resolution time-of-flight aerosol mass apectrometer, Atmos. Chem. Phys., 11, 1581–1602, doi:10.5194/acp-11-1581-2011, 2011.

Svenningsson, B., Rissler, J., Swietlicki, E., Mircea, M., Bilde, M., Facchini, M. C., Decesari, S., Fuzzi, S., Zhou, J., Mønster, J., and Rosenørn, T.: Hygroscopic growth and critical supersaturations for mixed aerosol particles of inorganic and organic compounds of atmospheric relevance, Atmos. Chem. Phys., 6, 1937–1952, doi:10.5194/acp-6-1937-2006, 2006.

Swietlicki, E., Hansson, H.-C., Hämeri, K., Svenningsson, B., Massling, A., McFiggans, G., McMurry, P. H., Petäjä, T., Tunved, P., Gysel, M., Topping, D., Weingartner, E., Baltensperger, U.,

Rissler, J., Wiedensohler, A., and Kulmala, M.: Hygroscopic properties of submicrometer atmospheric aerosol particles measured with H-TDMA instruments in various environments—a review, Tellus B, 60, 432–469, 2008.

Taha, G., Box, G. P., Cohen, D. D., and Stelcer, E.: Black carbon measurement using laser integrating plate method, Aerosol Sci. Technol., 41, 266–276, doi:10.1080/02786820601156224, 2007.

USEPA: Chemical Speciation Network Database, available at: http://views.cira.colostate.edu/fed/DataWizard/Default.aspx, last access: 1 December 2015

van Donkelaar, A., Martin, R. V, Brauer, M., and Boys, B. L.: Use of satellite observations for long-term exposure assessment of global concentrations of fine particulate matter, Environ. Health Perspect., 123, 135–143, doi:10.1289/ehp.1408646, 2015.

Varutbangkul, V., Brechtel, F. J., Bahreini, R., Ng, N. L., Keywood, M. D., Kroll, J. H., Flagan, R. C., Seinfeld, J. H., Lee, A., and Goldstein, A. H.: Hygroscopicity of secondary organic aerosols formed by oxidation of cycloalkenes, monoterpenes, sesquiterpenes, and related compounds, Atmos. Chem. Phys., 6, 2367–2388, doi:10.5194/acp-6-2367-2006, 2006.

Villalobos, A. M., Amonov, M. O., Shafer, M. M., Devi, J. J., Gupta, T., Tripathi, S. N., Rana, K. S., Mckenzie, M., Bergin, M. H., and Schauer, J. J.: Source apportionment of carbonaceous fine particulate matter (PM$_{2.5}$) in two contrasting cities across the Indo–Gangetic Plain, Atmos. Pollut. Res., 6, 398–405, doi:10.5094/APR.2015.044, 2015.

Vu Van, H., Le Xuan, Q., Pham Ngoc, H., and Luc, H.: Health risk assessment of mobility-related air pollution in Ha Noi, Vietnam, J. Environ. Prot. (Irvine, Calif.), 4, 1165–1172, 2013.

Wagner, F., Bortoli, D., Pereira, S., João Costa, M., Silva, A. M., Weinzierl, B., Esselborn, M., Petzold, A., Rasp, K., Heinold, B., and Tegen, I.: Properties of dust aerosol particles transported to Portugal from the Sahara desert, Tellus B, 61, 297–306, 2009.

Wang, J. L.: Mapping the global dust storm records: Review of dust data sources in supporting modeling/climate study, Curr. Pollut. Reports, 1, 82–94, doi:10.1007/s40726-015-0008-y, 2015.

Wang, Z., Chen, L., Tao, J., Zhang, Y., and Su, L.: Satellite-based estimation of regional particulate matter (PM) in Beijing using vertical-and-RH correcting method, Remote Sens. Environ., 114, 50–63, doi:10.1016/j.rse.2009.08.009, 2010.

Wexler, A. S. and Clegg, S. L.: Atmospheric aerosol models for systems including the ions H+, NH4+, Na+, SO$_4^{2-}$, NO$_3^-$, Cl$^-$, Br$^-$, and H$_2$O, J. Geophys. Res. Atmos., 107, ACH14–1–14, doi:10.1029/2001JD000451, 2002.

WHO: Human exposure to air pollution, in Update of the World Air Quality Guidelines World Health Organization, World Health Organization, Geneva, Switzerland, 61–86, 2005.

WHO: WHO Air quality guidelines – global update 2005, World Health Organization, Geneva, Switzerland, 2006.

Wise, M. E., Surratt, J. D., Curtis, D. B., Shilling, J. E., and Tolbert, M. A.: Hygroscopic growth of ammonium sulfate/dicarboxylic acids, J. Geophys. Res. Atmos., 108, 4638, doi:10.1029/2003JD003775, 2003.

Yang, F., Tan, J., Zhao, Q., Du, Z., He, K., Ma, Y., Duan, F., Chen, G., and Zhao, Q.: Characteristics of PM$_{2.5}$ speciation in representative megacities and across China, Atmos. Chem. Phys., 11, 5207–5219, doi:10.5194/acp-11-5207-2011, 2011.

Zhang, R., Jing, J., Tao, J., Hsu, S.-C., Wang, G., Cao, J., Lee, C. S. L., Zhu, L., Chen, Z., Zhao, Y., and Shen, Z.: Chemi-

cal characterization and source apportionment of PM$_{2.5}$ in Beijing: seasonal perspective, Atmos. Chem. Phys., 13, 7053–7074, doi:10.5194/acp-13-7053-2013, 2013.

Zhang, W.-J., Sun, Y.-L., Zhuang, G.-S. and Xu, D.-Q.: Characteristics and seasonal variations of PM$_{2.5}$, PM$_{10}$, and TSP aerosol in Beijing, Biomed. Environ. Sci., 19, 461–468, 2006.